Detailed Study of the 29 August 2018 Landslides on the Natural Hillside above Fan Kam Road, Pat Heung

GEO Report No. 363

AECOM Asia Company Limited

Geotechnical Engineering Office
Civil Engineering and Development Department
The Government of the Hong Kong
Special Administrative Region

[Blank Page]

Detailed Study of the 29 August 2018 Landslides on the Natural Hillside above Fan Kam Road, Pat Heung

GEO Report No. 363

AECOM Asia Company Limited

This report was originally produced in December 2019 as GEO Landslide Study Report No. LSR 2/2019

First published, December 2022

Prepared by:

Geotechnical Engineering Office,
Civil Engineering and Development Department,
Civil Engineering and Development Building,
101 Princess Margaret Road,
Homantin, Kowloon,
Hong Kong.

Preface

In keeping with our policy of releasing information which may be of general interest to the geotechnical profession and the public, we make available selected internal reports in a series of publications termed the GEO Report series. The GEO Reports can be downloaded from the website of the Civil Engineering and Development Department (http://www.cedd.gov.hk) on the Internet.

Raymond WM Cheung
Head, Geotechnical Engineering Office
December 2022

Foreword

This report presents the findings of a detailed study of landslide incidents (Incident Nos. 2018/08/2228 and 2018/08/2229) that occurred on a natural hillside above Fan Kam Road, Pat Heung during an intense rainstorm on 29 August 2018. The incidents primarily comprised three landslide clusters with total source volume ranging from 200 m^3 to 800 m^3. While the landslides initiated as open hillslope failures from multiple source areas within the landslide clusters, a number of which with debris converged into drainage lines and turned into channelised debris flows descending towards Fan Kam Road. The detached materials travelled a distance of about 300 m down the hillside, mostly coming to rest before reaching Fan Kam Road, but outwash debris inundated both lanes of the road resulting in temporary road closure among other consequences. The incidents were widely reported by the media. No casualties were reported.

The key objectives of the study were to document the facts about the landslides, present relevant background information and establish the probable causes of the landslides. The discussion and views expressed in this report are not intended to establish the existence of any duty at law on the part of the Government of the Hong Kong Special Administrative Region (HKSARG), its employees or agents, contractors, their employees or agents, or subcontractors, or any other party. This report neither determines nor implies liability towards any particular organization or individual except so far as necessary to achieve the said objectives.

The report was prepared for the Geotechnical Engineering Office of the Civil Engineering and Development Department, under Agreement No. CE 46/2015 (GE). This is one of a series of reports produced during the consultancy by AECOM Asia Company Limited. Unless otherwise agreed in writing, AECOM Asia Company Limited accepts no responsibility for any use of, or reliance on any contents of this Report by any person other than HKSARG or its employees or agents, and shall not be liable to any person other than HKSARG or its employees or agents, on any ground, for any loss, damage or expense arising from such use or reliance.

Patrick A Chao
Project Director
AECOM Asia Company Limited

Agreement No. CE 46/2015 (GE)
Study of Landslides Occurring in Kowloon and the New Territories between 2016 and 2018 - Feasibility Study

Contents

List of Tables

List of Figures

1 Introduction

During an intense rainstorm on 29 August 2018 when Landslip Warning was in effect, landslides in three distinct clusters (Incident Nos. 2018/08/2228 and 2018/08/2229), denoted as landslide clusters 2228, 2229U and 2229L, occurred on the natural hillside above Fan Kam Road, Pat Heung, with total source volume ranging from 200 m^3 to 800 m^3 (Figures 1.1). While the landslides initiated as open hillslope failures from multiple source areas within the landslide clusters, a number of which with debris converged into drainage lines and turned into channelised debris flows descending towards Fan Kam Road. The landslide debris mostly came to rest before reaching Fan Kam Road but outwash debris inundated both lanes of the road resulting in temporary road closure among other consequences. The incidents were widely reported by the media. No casualties were reported.

Following the incidents, AECOM Asia Company Limited (AECOM) carried out a detailed landslide study for the Geotechnical Engineering Office (GEO) of the Civil Engineering and Development Department (CEDD), under Agreement No. CE 46/2015 (GE).

The key objectives of the study were to document the facts about the landslides, present relevant background information and establish the probable causes of the landslides. This report presents the findings of the study which comprised the following key tasks:

(a) review of all known relevant documents relating to the site,

(b) aerial photograph interpretation (API),

(c) topographical surveys, detailed field observations and measurements,

(d) analysis of rainfall records,

(e) diagnosis of the probable mechanism and causes of the landslides, and

(f) diagnosis of the potential causes of the landslide clustering.

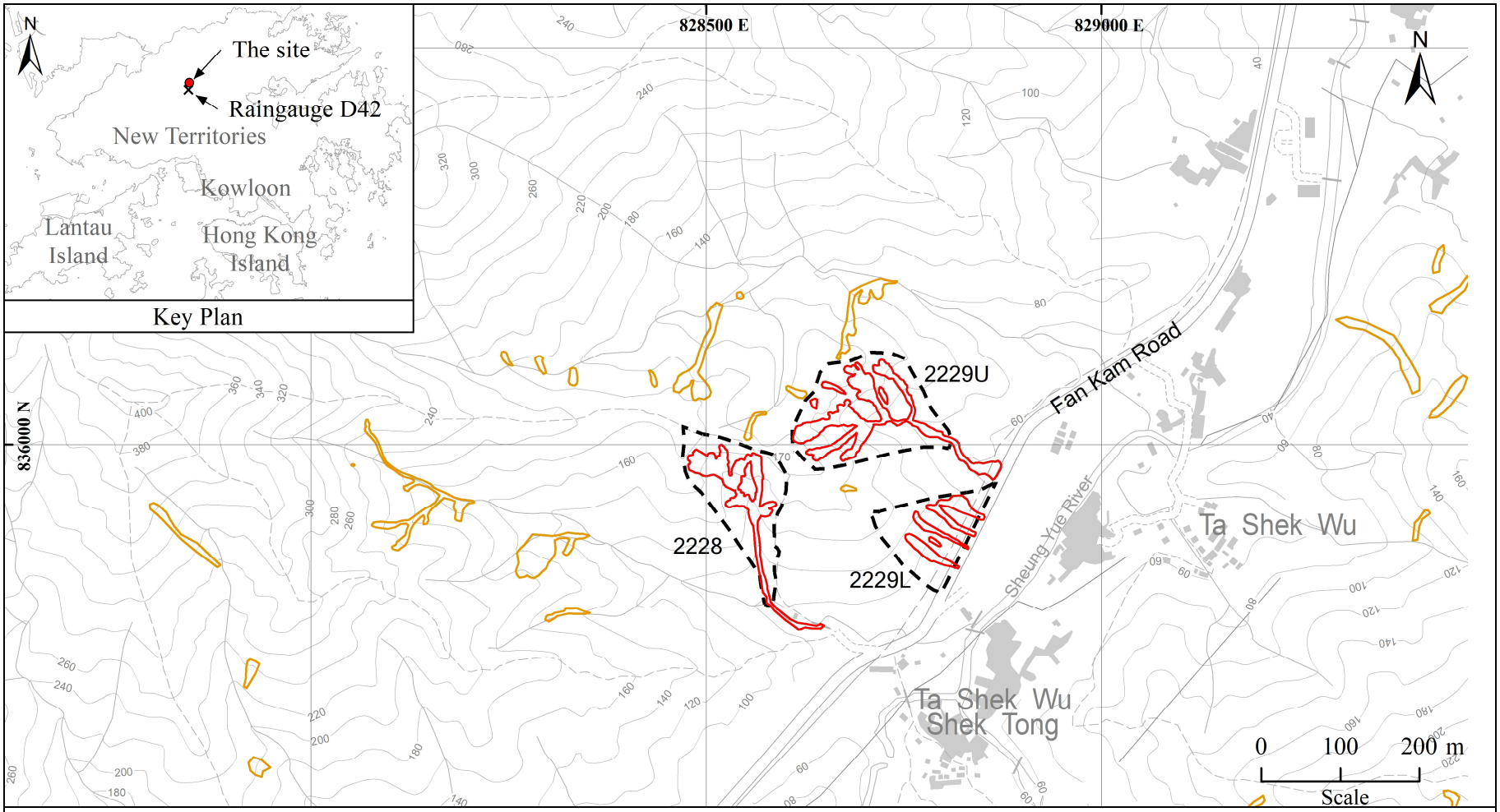

Figure 1.1 Location Plan

2 The Site

2.1 Site Description

The site is located in natural hillside catchments within the Lam Tsuen Country Park to the northwest of Fan Kam Road. The catchments in which the three landslide clusters developed, denoted as catchments 2228, 2229U and 2229L, are located at the lower portion of a spur descending from the summit of Kai Kung Leng at an elevation of about 585 mPD. Fan Kam Road is located at the toe of the hillside at an elevation of about 55 mPD. Further away from the toe of the hillside, Ta Shek Wu and Ta Shek Wu Shek Tong villages are at the opposite side of the road. The hillside is relatively steep and generally densely vegetated with shrubs (Figures 1.1 and 2.1).

Catchments 2228 and 2229U contain south- to southeast-trending incised perennial drainage lines which are fed by several ephemeral drainage lines on the valley flanks. These drainage lines drain down to Fan Kam Road and eventually converge into Sheung Yue River at further downstream. Catchment 2229L is located on a southeast-facing terrain with planar open hillslope setting immediate above Fan Kam Road with several ephemeral drainage lines.

2.2 Regional Geology

According to the Hong Kong Geological Survey (HKGS) 1:20 000 scale Solid and Superficial Geology Map Sheet No. 2 – San Tin (GCO, 1989) and Sheet No. 6 – Yuen Long (GCO, 1988), the site is underlain by coarse ash crystal tuff of the Tai Mo Shan Formation which is affected by regional dynamic metamorphism in northeast-trending belts across the areas (Figure 2.2). The three catchments are located within one of the metamorphic bands approximately 250 m wide, and the metamorphic effects are indicated to be increased imparted schistosity and increased in quartz content relative to the surrounding tuff (Langford et al, 1989). Foliation in the tuff is shown to dip southeast at about 30°. A northeast-trending regional Tai Lam Fault is located along Fan Kam Road, adjacent to the three catchments. Quartz veins are shown traversing a ridge on the valley opposite to landslide cluster 2228 at similar elevations. The HKGS 1:100 000 scale Pre-Quaternary Map Geology of Hong Kong (Sewell et al, 2000) also indicates that lapilli lithic bearing coarse ash crystal tuff of the Tai Mo Shan Formation underlies the site.

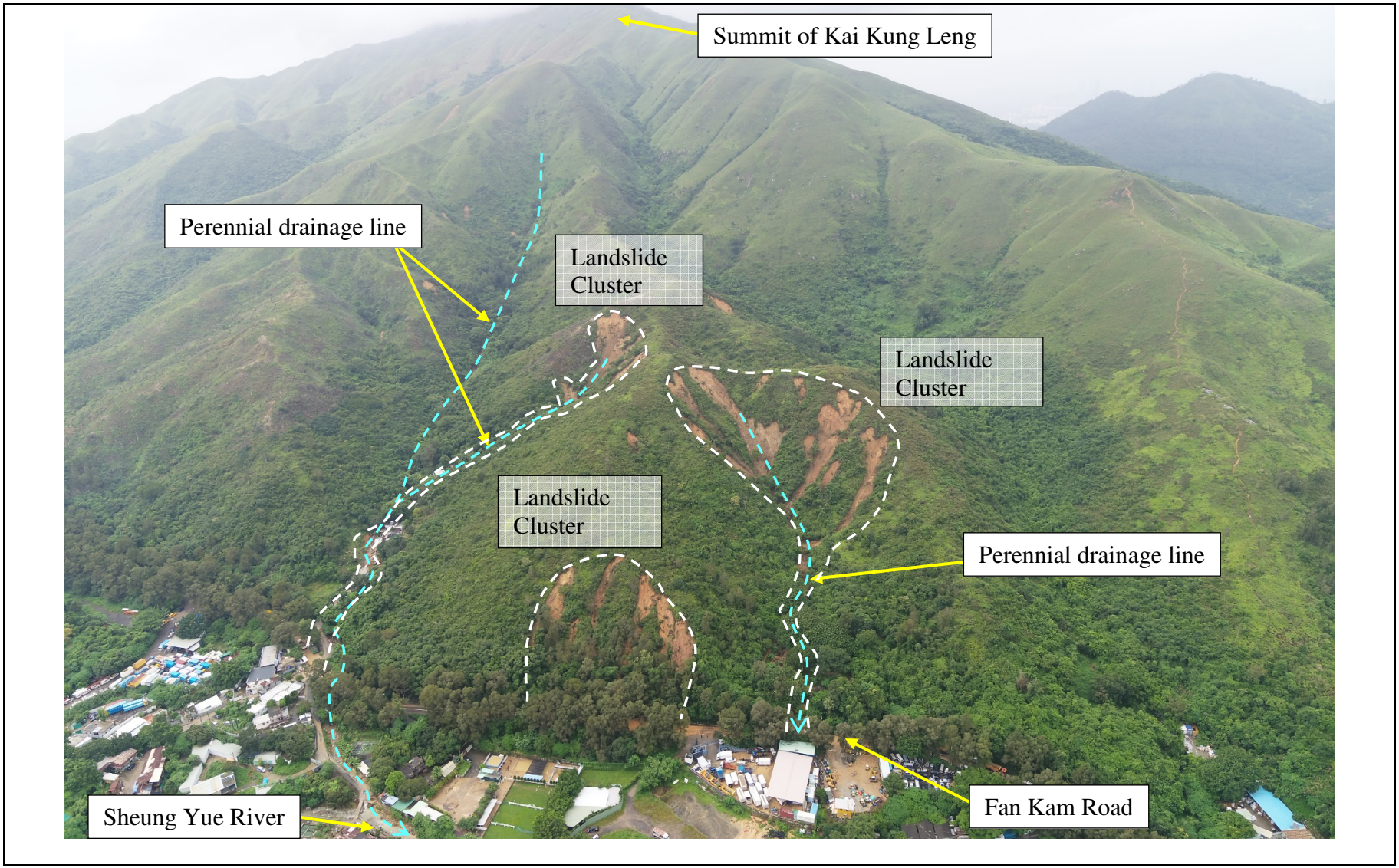

Figure 2.1 General View of the Landslides (Photograph taken on 30 August 2018)

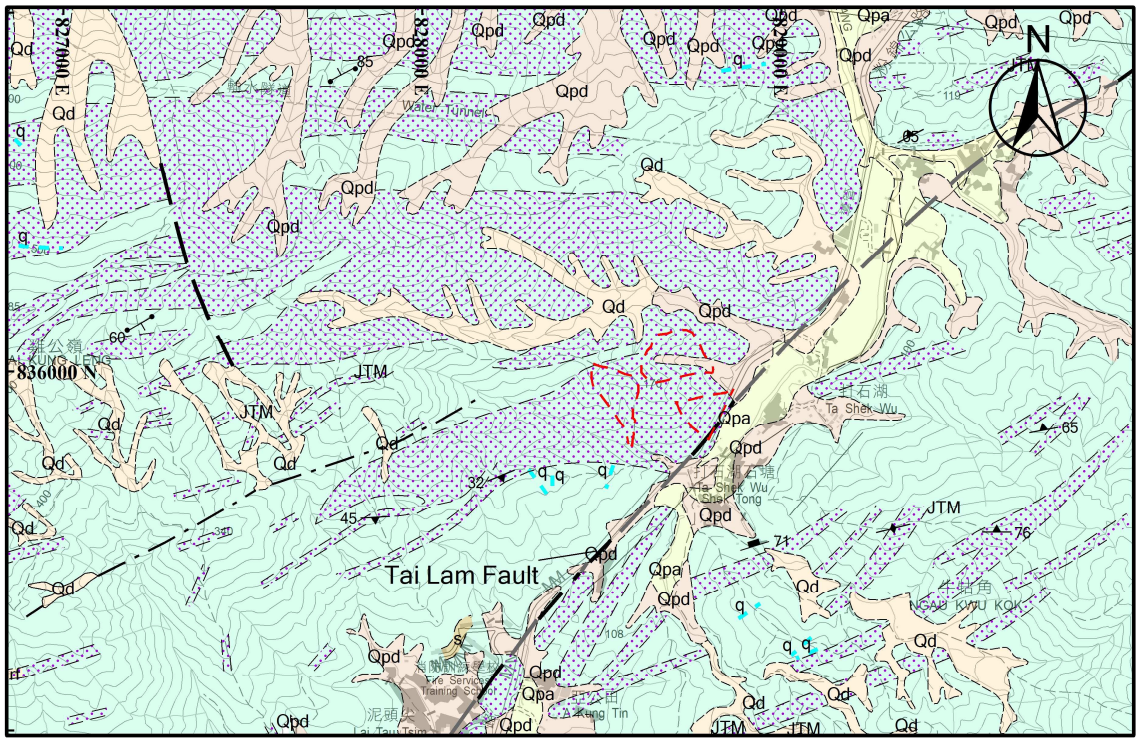

Legend:

- - - - Catchment boundary

Superficial deposits

Qa	Alluvium
Qd	Debris flow deposits
Qpa	Terraced alluvium
Qpd	Debris flow deposits

Solid geology

JTM	Coarse ash crystal tuff
s	Sandstone
rf	Feldsparphyric rhyolite
	Metamorphosed

Clay/silt, sand and gravel; well-sorted to semi-sorted

Unsorted sand, gravel, cobbles and boulders; clay/silt matrix

Clay/silt gravelly sandy; well-sorted to semi-sorted

Silt/sand, gravelly, clayey with cobbles and boulder; unsorted

0 200 400 m

Scale

Geological lines

------ Geological boundary, superficial deposits

– – – – Geological boundary, solid rock

— · — Photogeological lineament

—— – Fault

—— – Concealed Fault Note 2

– q – Mineral Vein

Structural symbols

20 Jointing

20 Inclined flow fabric

20 Inclined foliation

Vertical foliation

Notes:

(1) The map is extracted from Hong Geological Survey (HKGS), Map Series HGM 20, Sheet 2 (GCO, 1989) & Sheet 6 (GCO, 1988). 1:20 000 scale.

(2) The alignment of Tai Lam Fault concealed by superficial deposits is extracted form HKGS, Map Series HGM 100, Geological Map of Hong Kong, 1:100 000 scale (Sewell et al, 2000).

Figure 2.2 Regional Geology

3 Description of the Landslides

The following descriptions of the landslides have been collated mainly from records of the incidents from different government departments together with field observations.

The exact time of failure of the landslides is not known as no eyewitnesses can be found for the event. The Police records showed that the 999 call centre first received a report of landslides on Fan Kam Road adjacent to the landslide cluster areas at around 6:00 pm on 29 August 2018 from a member of the public. A section of Fan Kam Road between Pat Heung and Sheung Shui was completely closed from about 6:00 pm on 29 August 2018 to 7:20 am on 3 September 2018. Based on these records, the landslides probably occurred at some time before 6:00 pm on 29 August 2018 during the intense rainstorm.

The landslides forming the three landslide clusters notably comprise 36 individual landslide source areas (denoted as L1 to L36) in close proximity within catchments 2228, 2229U and 2229L (Figure 3.1). These source areas are generally located within steep terrain (typically 35° to 45°) between elevations of about 80 mPD and 170 mPD. Landslide clusters 2228 and 2229U are located within distinct topographic depressions draining into incised drainage lines, whilst landslide cluster 2229L is located on an open hillslope setting immediately above Fan Kam Road. Some isolated landslides are also noted on other parts of the hillside.

The landslides typically initiated as open hillslope failures from multiple sources areas within the landslide clusters. Debris from most of the source areas at landslide clusters 2228 and 2229U converged into drainage lines and became channelised debris flows descending towards Fan Kam Road, with a runout distance of about 300 m excluding outwash debris. The landslide debris mostly came to rest before reaching Fan Kam Road but outwash debris inundated both lanes of the road resulting in temporary road closure (Figures 3.2 and 3.3). The debris front, containing many boulders, impacted and blocked a cross-road culvert resulting in diversion of stream water and outwash over an access road incurring damage on several vehicles and a container (Figure 3.4). A storage structure adjoining a village house adjacent to the debris trail of landslide cluster 2228 was also reported to have been washed away (Figure 3.5).

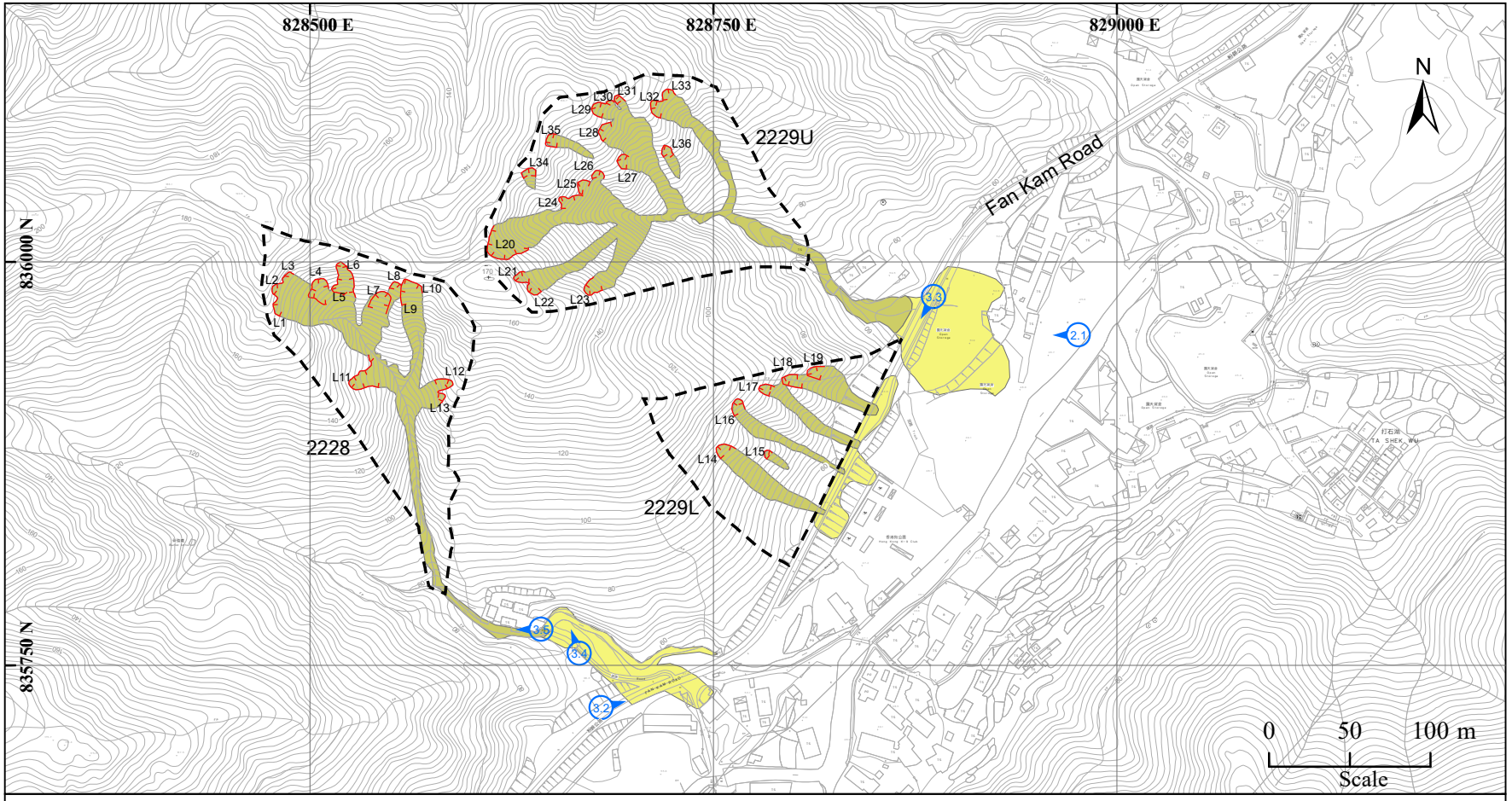

Figure 3.1 Site Layout Plan

Figure 3.2 View of Outwash Debris on Fan Kam Road from Landslide Cluster 2228 (Photograph taken on 30 August 2018)

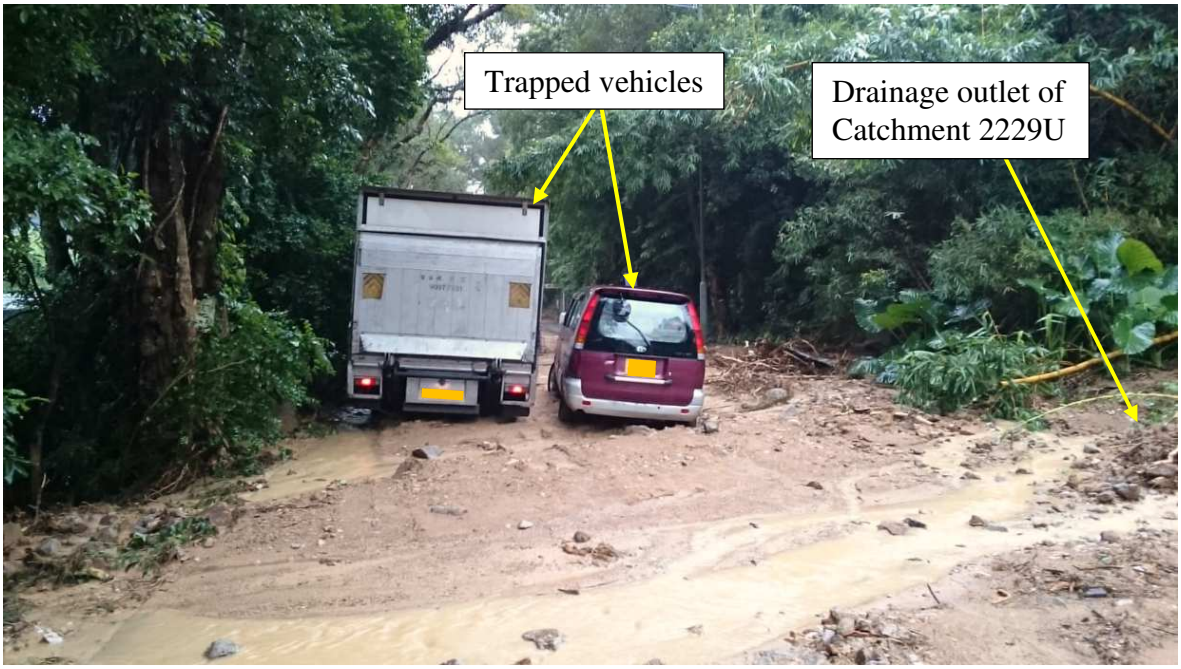

Figure 3.3 View of Outwash Debris on Fan Kam Road from Landslide Cluster 2229U (Photograph taken on 30 August 2018)

Figure 3.4 Damaged Vehicles and a Container (Photograph taken on 30 August 2018)

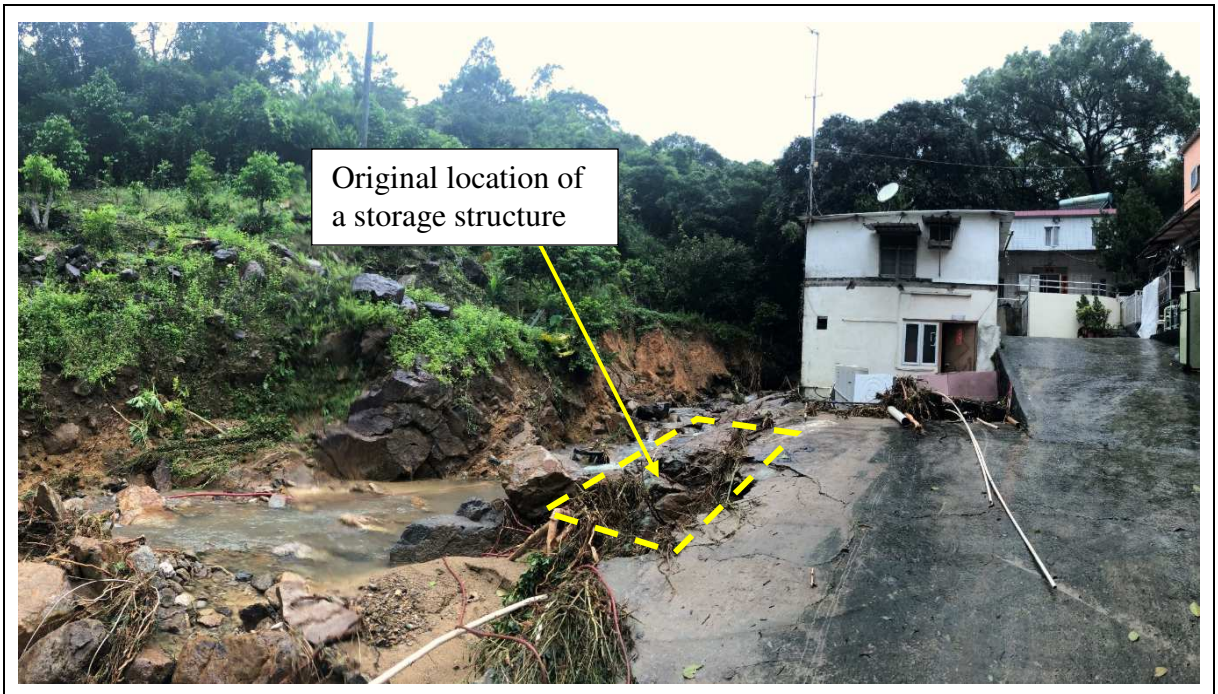

Figure 3.5 A Storage Structure Adjoining to Debris Trail of Landslide Cluster 2228 Reported to have been Washed Away (Photograph taken on 30 August 2018)

4 Site History and Past Instabilities

4.1 General

The site history and past instabilities have been determined from an interpretation of the available aerial photographs, together with a review of relevant documentary information (Figures 4.1 to 4.3). Detailed observations from the aerial photograph interpretation (API) are summarised in Appendix A, with the salient observations given below.

4.2 Site History

The site is located in natural hillside catchments above Fan Kam Road. The main anthropogenic activity observed in the vicinity is the construction of Fan Kam Road and associated slope formation at the toe of the hillside which was completed in 1954. Anthropogenic excavations in the form of elongated trenches and pits related to apparent military or mining activities are observed since 1954, located mainly on the ridgelines above catchments 2228 and 2229U.

The squatter structures located at the drainage outlet of catchment 2228 first appear in 1963. While by 1972, two other squatter structures are observed on a spurline about 30 m north of the outlet. Several more structures were constructed between 1992 and 2009 in the vicinity of the squatter structures that are first observed in 1963. At the drainage outlet of catchment 2229U, two squatter structures are first observed in 1972 and these structures appear to have been abandoned at the time of the 2018 landslides.

Catchments 2228, 2229U and 2229L and their vicinity have been frequently affected by hillfire. Hillfire events in 1973, 1975, 1981, 1993, 2003 and 2017 are identified. Predominantly the upper portions of catchments 2228 and 2229U were affected.

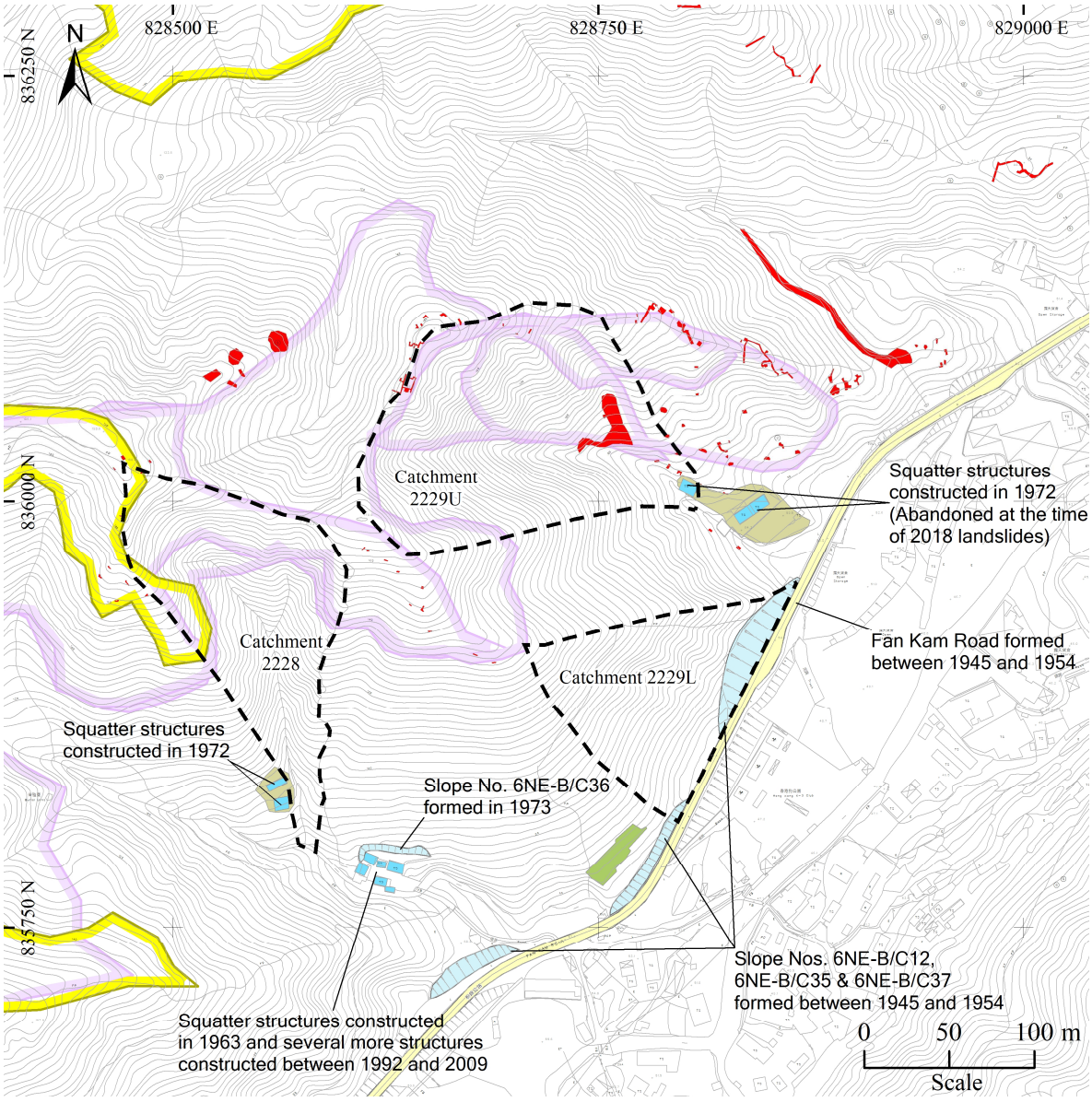

Legend:

- Catchment boundary
- Anthropogenic activities
  - Agricultural land
  - Low-rise structure
  - Site formation
  - Inferred excavation and disturbance
  - Fan Kam Road
  - Cut slope feature
- Approx. extent of hillfire affected area
  - Hillfire between 1973 and 2003
  - Hillfire in 2017

Note: Base plan is extracted from 1:1000 survey sheet Nos. 2SE-24D, 2SE-25C, 6NE-4B and 6NE-5A dated August 2014.

Figure 4.1 Site History

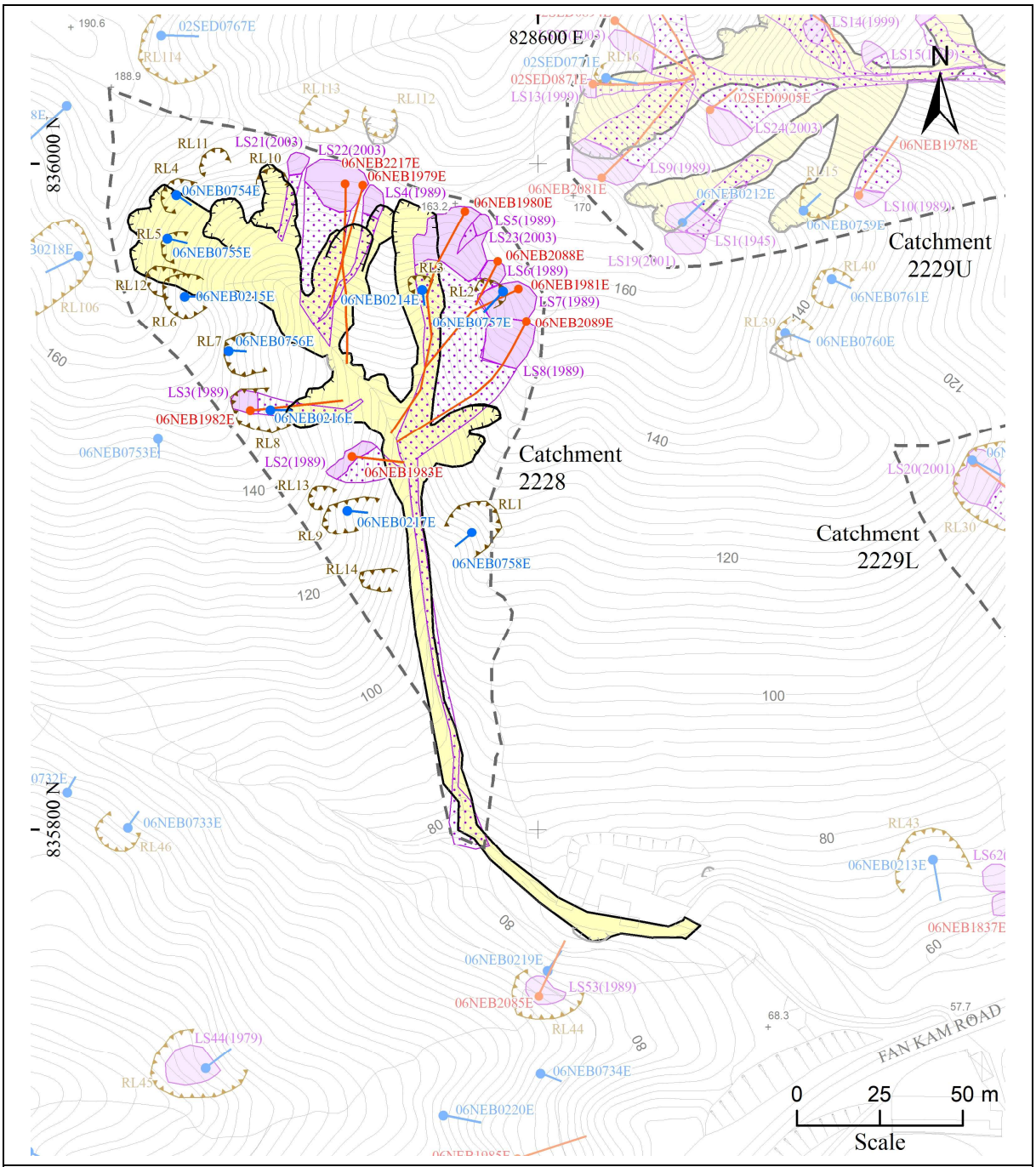

Legend:

	The 2018 landslide	06NED2200E	ENTLI (Recent)
	Catchment boundary	06NED2200E	ENTLI (Relict)
LS1 (year)	Recent landslide from API		Recent landslide debris from API
RL1	Relict landslide from API		

Note: Base plan is extracted from 1:1000 survey sheet Nos. 2SE-24D, 2SE-25C, 6NE-4B and 6NE-5A dated August 2014.

Figure 4.2 Past Instabilities at Catchment 2228

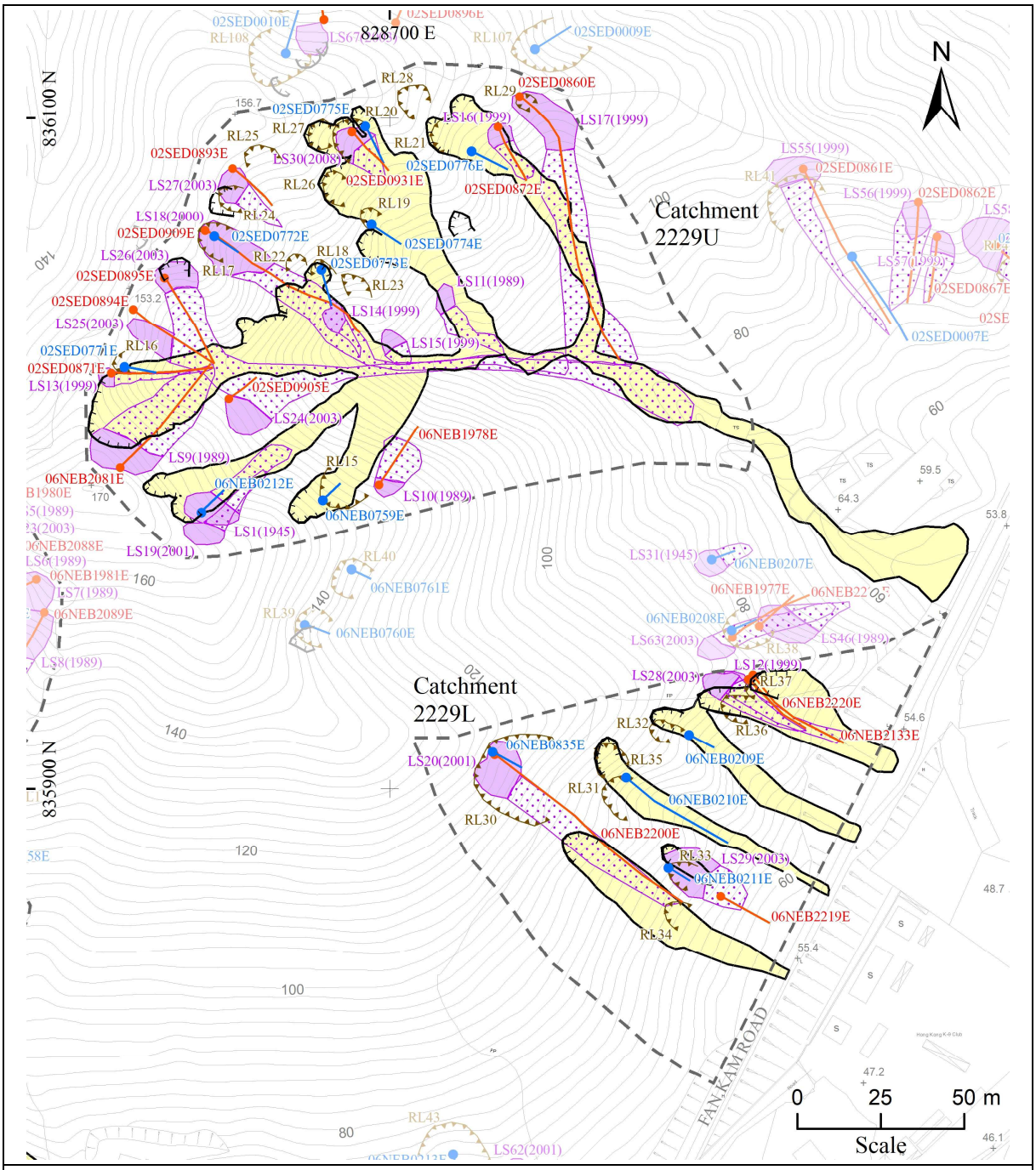

Legend:

	The 2018 landslide	06NED2200E	ENTLI (Recent)
	Catchment boundary	06NED2200E	ENTLI (Relict)
LS1 (year)	Recent landslide from API		Recent landslide debris from API
RL1	Relict landslide from API		

Note: Base plan is extracted from 1:1000 survey sheet Nos. 2SE-24D, 2SE-25C, 6NE-4B and 6NE-5A dated August 2014.

Figure 4.3 Past Instabilities at Catchments 2229U and 2229L

4.3 Past Instabilities at Catchments 2229U & 2229L

According to the Enhanced Natural Terrain Landslide Inventory (ENTLI), there are 21 relict and 23 recent landslides within the three catchments (Figures 4.2 and 4.3). Among these, nine relict and eight recent landslides locate within catchment 2228, eight relict and 11 recent landslides locate within catchment 2229U, and four relict and four recent landslides locate within catchment 2229L.

The detailed API conducted has identified some other past landslides in addition to those recorded in the ENTLI. In total, the three catchments contain 37 relict landslides (RL1 to RL37), of which 14 (RL1 to RL14) locate within catchment 2228, 15 (RL15 to RL29) locate within catchment 2229U and eight (RL30 to RL37) locate within catchment 2229L. These relict landslides are observed as shallow, rounded, degraded depressions predominately located at the heads of drainage lines or near the ridgelines, which are likely to be susceptible to retrogressive landslide action. Besides, a total of 30 recent landslides (LS1 to LS30) are identified within the three catchments. Among these, ten occurred within catchment 2228 in 1989 and 2003, 16 occurred within catchment 2229U between 1989 and 2008, and four occurred within catchment 2229L between 1999 and 2003. Most of the recent landslides in catchments 2228 and 2229U have the debris trails terminated before reaching the central main drainage lines, except for some of the landslides in 1989 and 2003 which converged into the drainage lines and turned into channelised debris flows with a runout distance of about 200 m.

The three catchments have experienced frequent historical landslides and the debris are generally observed to have spread on the hillside or accumulated along the valley. No debris lobe of significant size is observed throughout the aerial photographic records. Besides, no significant signs of erosion or instability are identified in the three catchments since 2008.

No relevant landslide data within the three catchments are found in the GEO's Large Landslide Database (Scott Wilson, 1999) and Landslide Report Database System.

5 Post-failure Observations and Landslide Process

5.1 General

The landslides within the three landslide clusters were initially inspected by AECOM on 30 August 2018. Subsequently, several field inspections and mapping were carried out over the next few months.

The landslides (L1 to L36), forming three landslide clusters, are relatively shallow (generally less than 1 m in depth) and the majority of which are situated adjacent to heads of drainage lines and past landslide locations, and below ridgelines. The width of the source areas varies from about 5 m to 22 m, with an average width of about 8 m. Estimated source area failure volumes range from about 10 m^3 to 240 m^3, with thin patches of debris remaining on many of the source floors. In most of the source areas inspected, the majority of materials exposed in the main scarp are colluvium with the surface of rupture primarily along or proximate to an interface between the colluvium and weathered tuff. The predominant failed materials are colluvium with minor amounts of completely to highly decomposed tuff (C/HDT). Highly to moderately decomposed tuff (H/MDT) was partially exposed in many of

the source floors and some contained continuous quartz veins over several meters. None of the landslides are found to have been controlled structurally by the presence of quartz (viz. the quartz veins are generally not dipping out of the slope). Extensive quartz fragments were observed on the ground surface along the ridgelines above landslide clusters 2228 and 2229U. A summary of the characteristics of the landslides is presented in Table 5.1.

As these landslides predominantly involved detachment of colluvium, a large proportion of the observed debris along the trail comprises rock and quartz fragments within a fine matrix of sandy silt. Patches of remoulded debris were observed along the debris trails of landslide clusters 2228 and 2229U, some of which were deposited as levees higher up on the flanks, which was considered as evidence of debris flow process. Some lobes of debris deposition were observed especially at confluences of drainage lines from individual source areas. Outwash debris comprising mainly sorted silty sand with some gravels were observed extending into Fan Kam Road probably due to post-failure erosion and transportation of landslide debris by surface runoff and stream overflow.

Plans of the three landslide clusters are shown in Figures 5.1 and 5.2. Longitudinal sections of landslide clusters 2228 and 2229U, which involve channelised debris flows, are presented in Figures 5.3 and 5.4, with associated landslide mapping plans shown in Appendix B.

The following sections present salient observations from the detailed mapping of the three landslide clusters.

Table 5.1 Key Data Pertaining to the Source Areas of the Landslide Clusters

Landslide No.	Catchment	Width W (m)	Length L (m)	Depth D (m)	Estimated Source Volume (m^3)	Pre-failure Slope Gradient (Degrees)	Predominant Failed Materials	Underlying Regolith Type
L1	2228	10	8	0.7	27	39	Coll	Sv (III/IV)
L2	2228	10	15	0.7	53	41	Coll	Sv (III/IV)
L3	2228	8	13	0.7	37	41	Coll	Sv (III/IV)
L4	2228	12	14	0.7	62	31	Coll	Sv (IV)
L5	2228	5	6	0.7	10	41	Coll	Sv (IV)
L6	2228	9	26	0.6	74	39	Coll	Sv (IV)
L7	2228	10	16	0.7	59	36	Coll	Sv (III/IV)
L8	2228	5	6	0.6	8	38	Coll	Sv (III/IV)
L9	2228	6	15	0.6	28	35	Coll	Sv (III/IV)
L10	2228	7	14	0.6	31	36	Coll	Sv (III/IV)
L11	2228	11	24	0.9	119	29	Coll	Sv (IV)
L12	2228	8	12	0.7	33	37	Coll	Sv (IV)
L13	2228	6	7	0.6	12	42	Coll	Sv (IV)
Average	-	8	13	0.7	42	37	-	-
L14	2229L	11	9	0.8	44	33	Coll	Sv (IV)
L15	2229L	5	6	0.8	12	39	Coll	Sv (IV)
L16	2229L	8	11	0.8	35	37	Coll	Sv (IV)
L17	2229L	7	10	0.8	29	35	Coll	Sv (IV)
L18	2229L	8	15	0.8	51	33	Coll	Sv (IV)
L19	2229L	9	12	0.8	44	35	Coll	Sv (IV)
Average	-	8	10	0.8	36	35	-	-
L20	2229U	22	25	0.8	235	37	Coll	Sv (IV)
L21	2229U	7	15	0.8	42	40	Coll	Sv (III/IV)
L22	2229U	8	10	0.7	30	44	Coll	Sv (III/IV)
L23	2229U	10	15	0.8	61	39	Coll	Sv (IV)
L24	2229U	11	17	0.7	68	42	Coll	Sv (III/IV)
L25	2229U	9	11	0.7	38	42	Coll	Sv (IV) + Rt
L26	2229U	8	8	0.7	23	43	Coll	Sv (III/IV)
L27	2229U	8	11	0.7	33	42	Coll	Sv (IV)
L28	2229U	10	11	0.8	41	41	Coll	Sv (IV)
L29	2229U	9	12	0.8	44	38	Coll	Sv (IV) + Rt
L30	2229U	5	5	0.8	8	41	Coll	Rt
L31	2229U	5	10	0.8	18	38	Coll	Sv (IV)
L32	2229U	11	12	0.8	53	38	Coll	Sv (IV) + Rt
L33	2229U	9	9	0.8	33	36	Coll	Sv (IV)
L34	2229U	9	10	0.6	28	52	Coll	Sv (IV)
L35	2229U	8	9	0.8	31	37	Coll	Sv (IV)
L36	2229U	7	14	0.8	39	40	Coll	Sv (IV)
Average	-	9	12	0.8	49	40	-	-
Overall Average	-	8	12	0.7	44	38	-	-

Regolith legend: Coll – Colluvium, Sv – Weathered tuff (weathering grade shown in bracket), Rt – Intermittent tuff outcrop

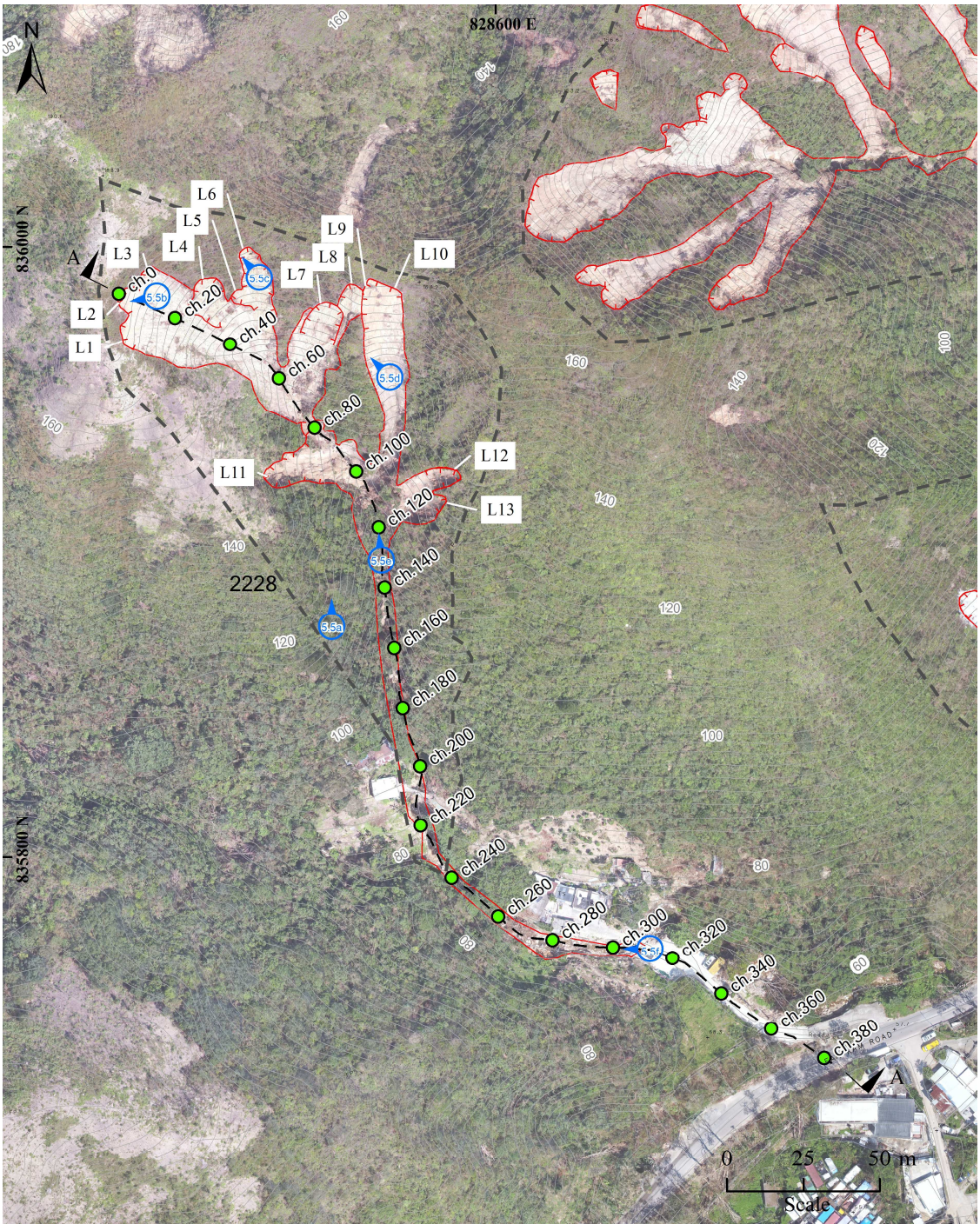

Legend:

The landslide main scarp — — — Catchment boundary The landslide

Location and direction of photograph as shown in Figure 5.5a

Note: Base plan is extracted from 1:1000 survey sheet Nos. 2SE-24D, 2SE-25C, 6NE-4B and 6NE-5A dated August 2014.

Figure 5.1 Plan of Landslide Cluster 2228

Legend:

The landslide main scarp — — — Catchment boundary The landslide

Location and direction of photograph as shown in Figure 5.6a

Note: Base plan is extracted from 1:1000 survey sheet Nos. 2SE-24D, 2SE-25C, 6NE-4B and 6NE-5A dated August 2014.

Figure 5.2 Plan of Landslide Clusters 2229U and 2229L

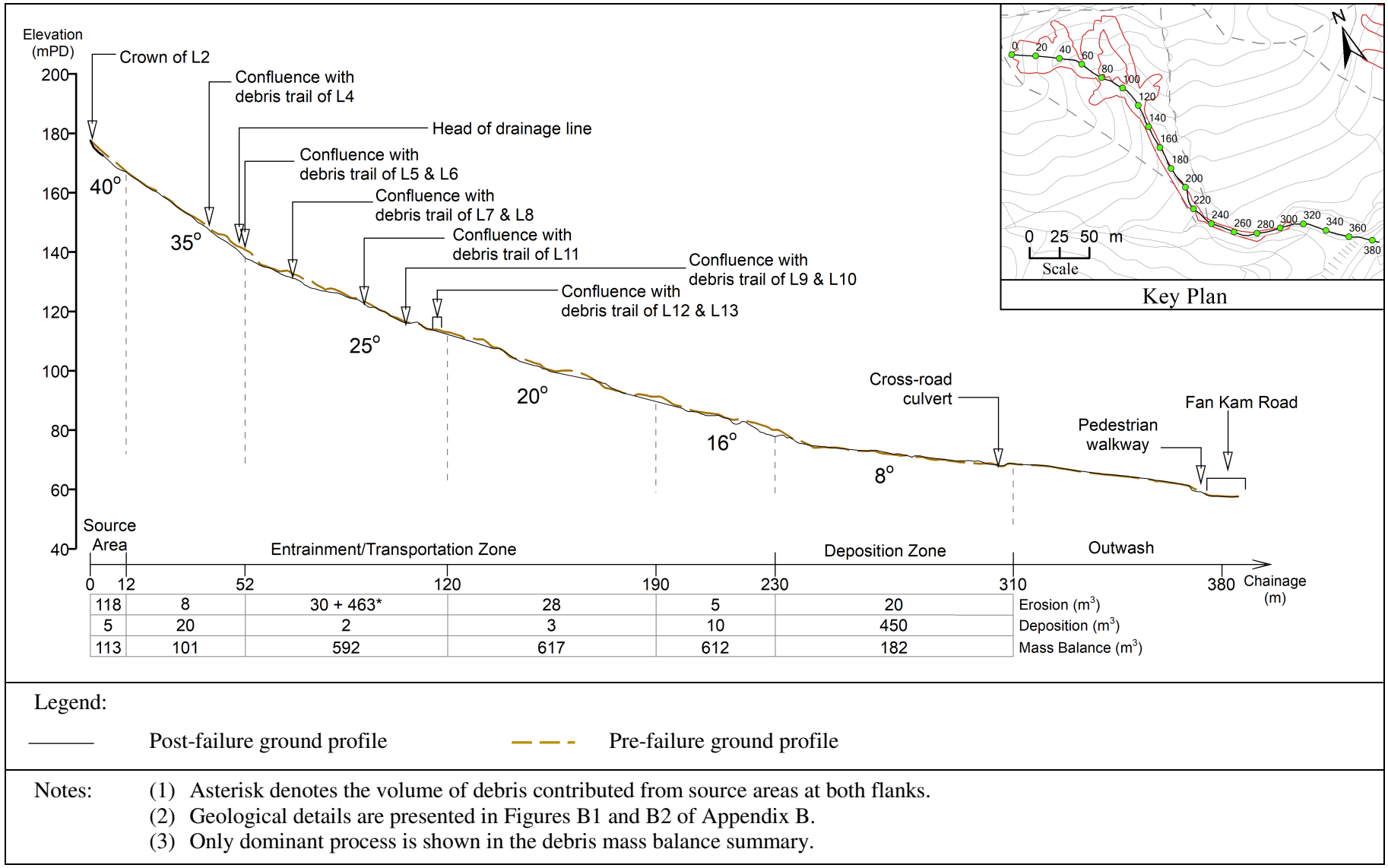

118	8	30 + 463*	28	5	20	Erosion (m^3)
5	20	2	3	10	450	Deposition (m^3)
113	101	592	617	612	182	Mass Balance (m^3)

Legend:

——— Post-failure ground profile — — — Pre-failure ground profile

Notes:
(1) Asterisk denotes the volume of debris contributed from source areas at both flanks.
(2) Geological details are presented in Figures B1 and B2 of Appendix B.
(3) Only dominant process is shown in the debris mass balance summary.

Figure 5.3 Longitudinal Section A-A through Landslide Cluster 2228

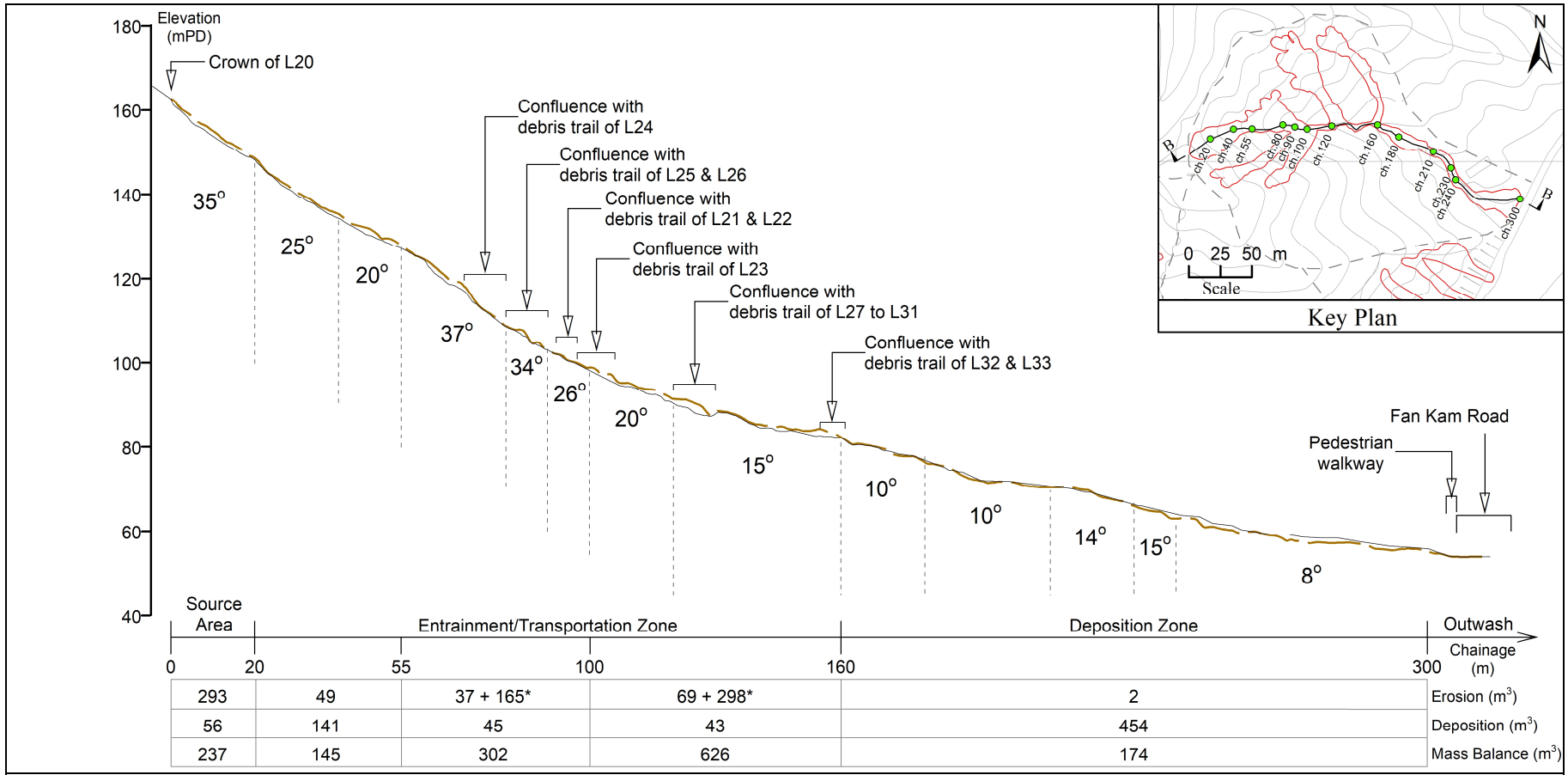

293	49	37 + 165*	69 + 298*	2	Erosion (m^3)
56	141	45	43	454	Deposition (m^3)
237	145	302	626	174	Mass Balance (m^3)

Legend:

——— Post-failure ground profile — — — Pre-failure ground profile

Notes:
(1) Asterisk denotes the volume of debris contributed from source areas at both flanks.
(2) Geological details are presented in Figures B3 and B4 of Appendix B.
(3) Only dominant process is shown in the debris mass balance summary.

Figure 5.4 Longitudinal Section B-B through Landslide Cluster 2229U

5.2 Landslide Cluster 2228 (Channelised Debris Flow)

Landslide cluster 2228 is located within a distinct topographic depression and comprises 13 source areas, namely L1 to L13, some of which are adjoined and form five separate debris trails before converging into the central main drainage line of the catchment (Figure 5.5a). The source areas are generally located within the steep terrain of the upper catchment, and are relatively shallow with an average failure depth of about 0.7 m, giving a total estimated volume of detached materials of about 550 m^3 (Table 5.1). The maximum active volume of the channelised debris flow taken into account the material entrainment and deposition is about 620 m^3 (Figure 5.3).

The materials exposed within the main scarps, indicating the detached materials, are mainly colluvium comprising firm to stiff, yellowish brown, sandy silt with some fine to coarse gravel-sized tuff and occasional quartz fragments, overlying minor amounts of C/HDT. Failures generally occurred along the interface between colluvium and underlying weathered tuff (Figure 5.5b). Many source areas have significant proportion of H/MDT exposed in the source floor, where discontinuous joint surfaces were observed, some of which are dipping parallel to the slope (Figure 5.5c), although the persistence is insufficient to control failure. Quartz veins up to 80 mm thick and continuous over two to three meters were observed within some of the source areas which are generally dipping into the slope. Noting that many of the source areas were covered by remoulded debris limiting the exposure, it is anticipated that the actual extent of quartz veins within the source areas could be greater. Soil pipes (generally 25 mm to 100 mm diameter) were observed in many of the main scarps, particularly at the interface of colluvium and weathered tuff. Several minor tension cracks were observed around the main scarps of some of the landslides and could not be traced more than a few metres from the main scarps. These cracks are probably associated with the recent instability since the cracks are free of vegetation.

The debris trail up to about Chainage 60 is not confined with trail width up to 10 m and generally sloping between 25° and 35°. About 20 m^3 of debris was deposited along the debris trail at this section as remoulded debris, comprising gravel- and cobble-sized clasts within a sandy silt matrix, forming elongated lobes or levees on the periphery of the trail (Figure 5.5d). From Chainage 60 to 230, the debris trail becomes incised with a gradient of between 20° and 25°. Relatively little entrainment (< 35 m^3) was observed but significant areas of flow-aligned vegetation and superficially eroded topsoil was observed on the flanks of the debris trails indicating the dominant process is transportation (Figure 5.5d). Coarse ash tuff outcrops were often observed in the debris trail bed and flanks and contain persistent multiple veins of quartz up to 100 mm thick (Figure 5.5e). The limited entrainment appears to be due to a lack of entrainable materials within the drainage line prior to failure as evidenced by flow-aligned remnant vegetation on the rock surfaces. No superelevation marks could be observed.

(a) General View of Source Areas of Landslide Cluster 2228

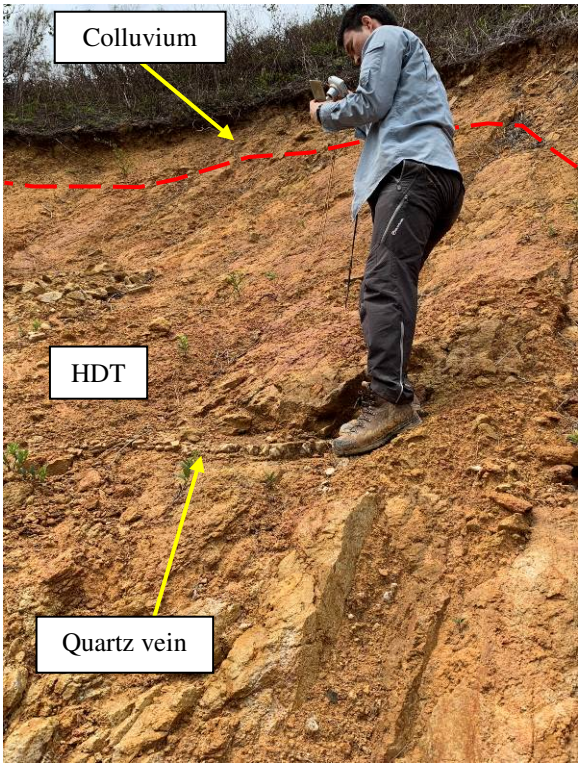

(b) View of L2 Showing Predominant Materials of the Landslides

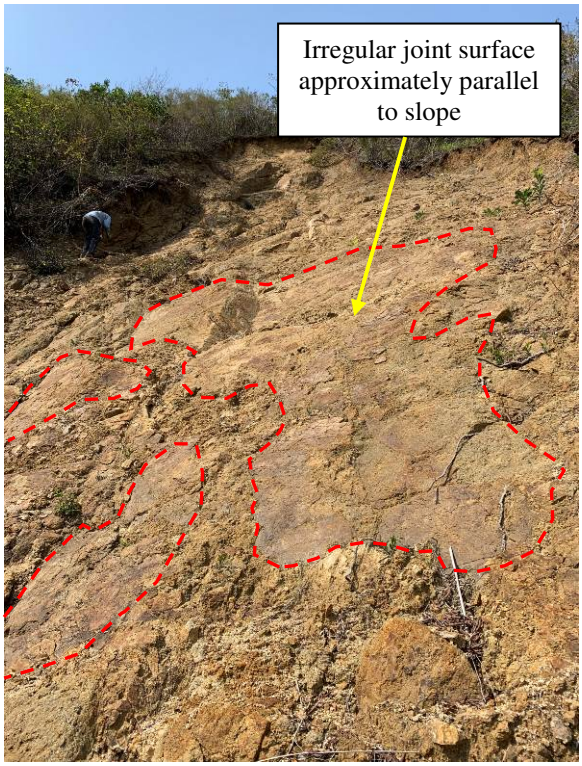

(c) View of L6 Showing Rock Forming Part of Source Floors

Figure 5.5 Key Observations of Landslide Cluster 2228 (Photographs taken on 30 August 2018 and 12 March 2019) (Sheet 1 of 2)

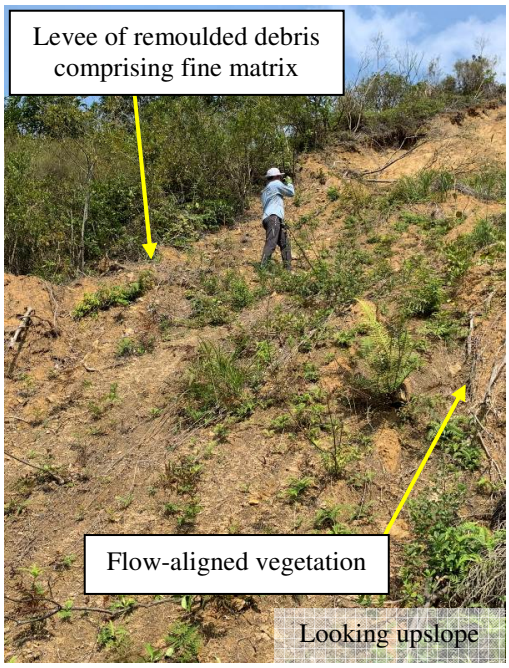

(d) View of Debris Trail of L10 at CH100 Showing Transportation Process

(e) View of Debris Trail from CH130 to CH140 Showing Rocky Stream Bed with Minor Erosion

(f) General View of End of Debris Trail at CH310

Figure 5.5 Key Observations of Landslide Cluster 2228 (Photographs taken on 30 August 2018 and 12 March 2019) (Sheet 2 of 2)

The gradient of the debris trail decreases to about 8° at Chainage 230 where it merges with a perennial stream course draining a large catchment above the landslides. The debris trail is less confined with about 450 m^3 of deposition of both remoulded and clastic debris. Post-event fluvial erosion of the debris from the stream course discharge is evident, forming downstream outwash. At Chainage 310, a significant proportion of cobbles, large boulders and tree branches was observed (Figure 5.5f) which likely formed the debris front, completely blocking a cross-road culvert. The blockage of the cross-road culvert consequently diverted the stream flow and outwash debris onto the access road where it deposited as sorted sand and gravel with cobbles and boulders that were pushed down by the significant water flow, damaging several parked vehicles and a container. The deposition of fine-grained fluvial outwash debris continued for a further 100 m downslope, reaching Fan Kam Road and continuing to flow and deposit northwards along the road (Figure 3.2).

5.3 Landslide Cluster 2229U (Channelised Debris Flow)

Landslide cluster 2229U is located within a distinct topographic depression and comprises 17 source areas, namely L20 to L36, 14 of which resulting in six separate debris trails before converging into the central main drainage line (Figure 5.6a). The source areas are generally located within the steep terrain below the ridgelines and spurs with slope gradient between 35° and 40°. The largest source area (i.e. L20) has a detached volume of approximately 300 m^3 and a total estimated volume of detached materials is about 800 m^3 (Table 5.1). The maximum active volume of the channelised debris flow taken into account the material entrainment and deposition is about 630 m^3 (Figure 5.4).

Failures generally occurred along the interface between colluvium and underlying weathered tuff. Similar to landslide cluster 2228, the materials exposed within the main scarps in landslide cluster 2229U are mainly colluvium comprising firm to stiff, yellowish brown and brown, sandy silt with some gravel-sized tuff and quartz fragments. The average failure depth is about 0.8 m, locally up to 1.0 m (Figure 5.6b). Some of the source areas have a significant proportion of H/MDT exposed in the source floors. Some exposed joints were observed to be locally daylighting or occasionally forming wedge geometry within the rupture surface (Figure 5.6c). All the joint surfaces are irregular over short distances and have low persistence (less than 3 m), and hence they are unlikely to control the failure.

Several bands of persistent quartz veins up to 200 mm thick could be locally observed at source areas L25 and L26, which are generally dipping into the rupture surface (Figures 5.6c). Some quartz veins of about 10 mm thick are also present at source area L31 which are likely to be quartz infill along joints. Similar to landslide cluster 2228, soil pipes (generally 50 mm to 100 mm diameter) with minor infilling of silty sand and several minor tension cracks were occasionally observed in the main scarps of some of the landslides.

Below source area L20 and up to Chainage 160, transportation is the dominant process with little erosion or deposition. The debris trail at this section is generally sloping between 25° to 35° with local 'steps' in the drainage profile. Patches of coarse ash tuff outcrops are commonly exposed at the base of drainage channel and the eroded colluvial deposits are exposed on the flanks of the incised channel. The observations of the presence of flow-aligned vegetation on the flanks of the debris trails and the rocky substrate (Figure 5.6d)

suggest that the amount of entrained materials is relatively modest (about 150 m^3). With relatively little overall deposition in the debris trail (about 90 m^3), most of the debris continued downstream. Below Chainage 160, the slope angle reduced to about 10° and the channel becomes less incised, with some relatively flat terrace-like areas along the drainage line. The change in drainage line morphology and slope angle resulted in the onset of significant deposition. Between Chainage 160 and 300, about 450 m^3 of remoulded debris and coarse clastic debris was deposited (Figure 5.6e). Abandoned structures at approximately Chainage 210 and 260 appear to have been destroyed or damaged by the debris flow. At Chainage 300 just before reaching the Fan Kam Road, a significant proportion of cobbles and boulders was observed which likely formed the debris front (Figure 5.6f).

Outwash debris mainly comprising water sorted silty sand and gravel was observed on Fan Kam Road and further downslope, which had been transported by post-failure fluvial processes (Figure 3.3).

(a) General View of Source Areas of Landslide Cluster 2229

Figure 5.6 Key Observations of Landslide Cluster 2229U (Photograph taken on 30 August 2018) (Sheet 1 of 3)

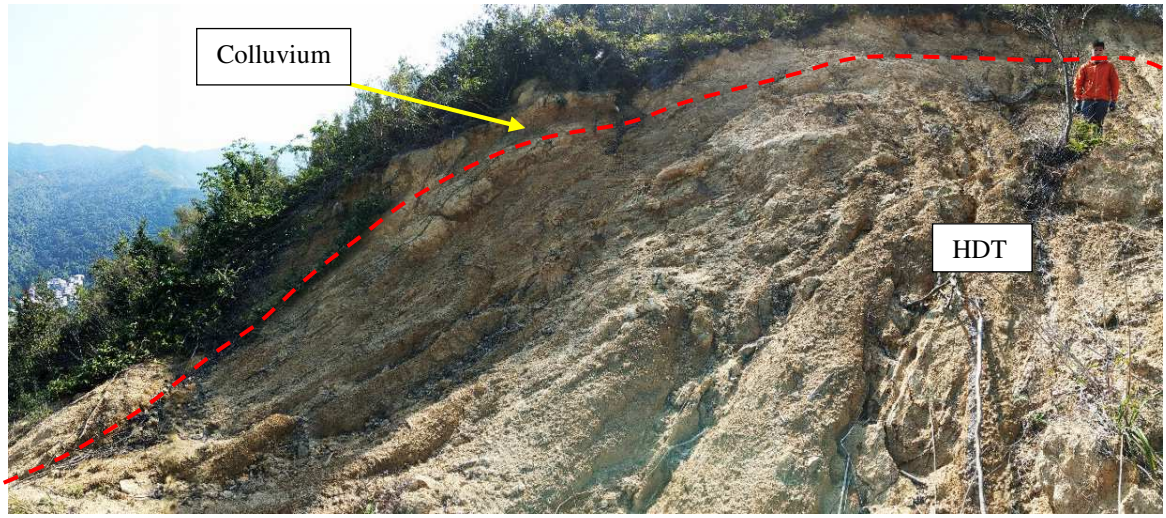

(b) View of L20 Showing Predominant Materials of the Landslides

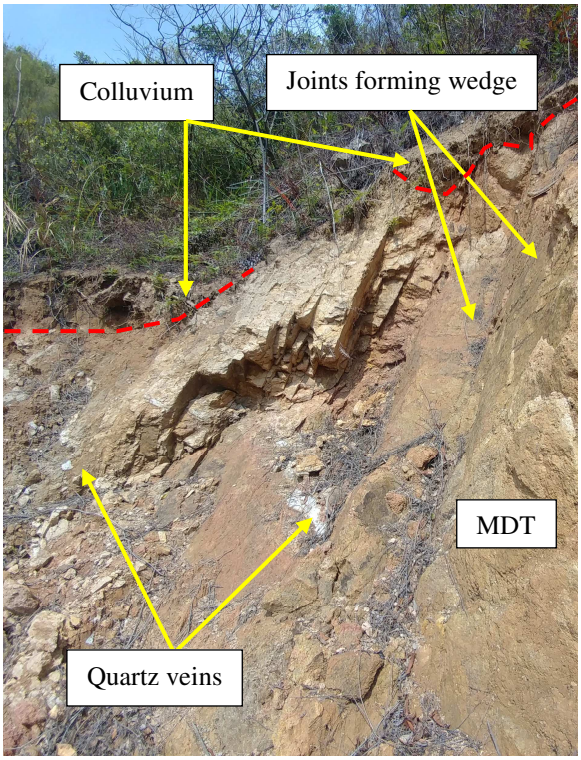

(c) View of L25 and L26 Showing Quartz Veins and Rock Joints Forming Wedge

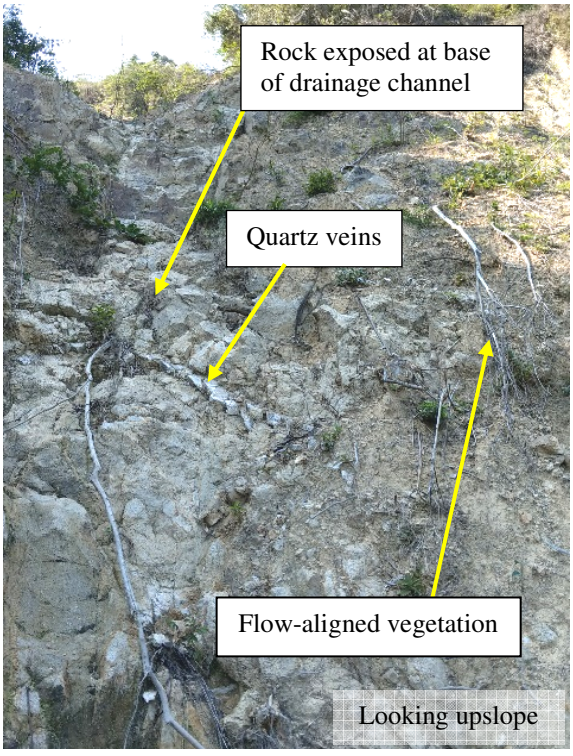

(d) View of Debris Trail from CH60 to CH80 Showing Transportation Process

Figure 5.6 Key Observations of Landslide Cluster 2229U (Photographs taken on 30 August 2018 and 24 January 2019) (Sheet 2 of 3)

(e) View of Debris Trail from CH190 to CH200 Showing the Deposition Zone

(f) General View Near the End of Debris Trail

Figure 5.6 Key Observations of Landslide Cluster 2229U (Photographs taken on 30 August 2018) (Sheet 3 of 3)

5.4 Landslide Cluster 2229L (Open Hillslope Failure)

Landslide cluster 2229L comprises three distinct source areas (L14 to L16) and three adjoined source areas (L17 to L19), and being open hillslope failures, most of them appear to spread and coalesce downslope (Figure 5.7a). The source areas are located within a steep open hillslope terrain (typically 35° and 40°) directly above a cut slope (Feature No. 6NE-B/C12) adjacent to Fan Kam Road (Figure 5.2). The source areas are relatively shallow with an average failure depth of about 0.8 m, giving a total estimated volume of detached materials of about 200 m^3.

The materials exposed within the main scarps composed of mainly colluvium, which comprises firm to stiff, yellowish brown and brown, sandy silt with some fine to coarse gravel, with minor C/HDT. Patches of H/MDT are exposed in most of the source areas (Figure 5.7b). Soil pipes and quartz veins up to 20 mm thick were locally observed within source areas and gravel-sized quartz fragments were observed within the landslide debris.

The landslide debris mostly comprises yellowish brown, silty sand with some occasional cobble-sized rock fragments and vegetation debris. Although some vegetation is entrained within the debris, some of the more robust trees remain on the debris trail giving an indication of the debris height from the abrasion marks (Figure 5.7c). These open hillslope failures differ from the debris flow events of landslide clusters 2228 and 2229U in that the travel distance is relatively short and most of the debris formed distinct lobes on Fan Kam Road (Figure 5.7d), although some could still be observed on the sloping ground above the cut slope (Figure 5.7e).

(a) General View of Source Areas of Landslide Cluster 2229L

Figure 5.7 Key Observations of Landslide Cluster 2229L (Photograph taken on 30 August 2018) (Sheet 1 of 2)

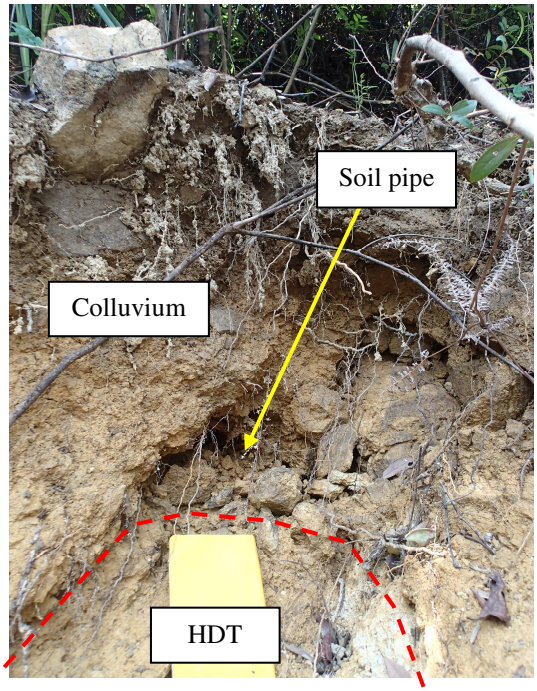

(b) View of L14 Showing Predominant Materials of the Landslides

(c) Abrasion Marks on Tree Along Debris Trail Indicating the Maximum Debris Height

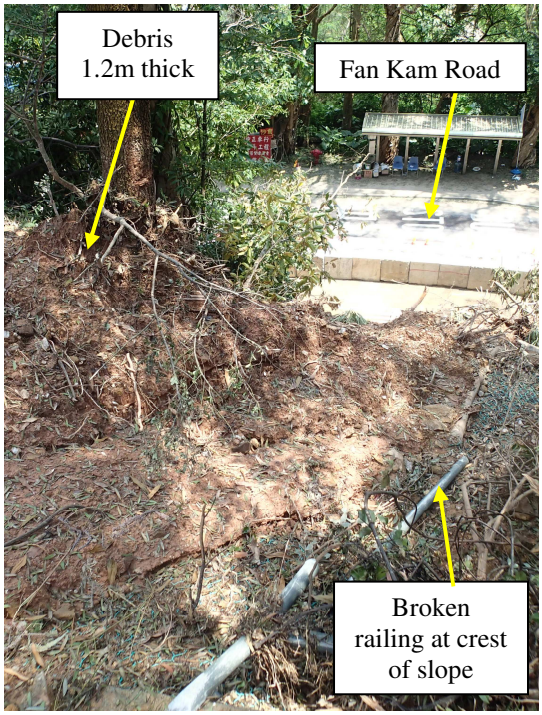

(d) View of Debris Trail Showing Debris Deposition on the Crest of Cut Slope

(e) View of Landslide Debris deposited on Fan Kam Road

Figure 5.7 Key Observations of Landslide Cluster 2229L (Photographs taken on 30 August 2018) (Sheet 2 of 2)

6 Geomorphology and Geology

The terrain forming the three catchments for which the three landslide clusters developed is characterised by steep slopes (Figure 6.1). Around 50% of the areas of these catchments comprise terrain with gradient greater than 35°, being much higher than that of the territory-wide natural terrain areas in Hong Kong (viz. approximately 16% with reference to Lo et al (2015)). For the source areas of the 2018 landslides, about 80% of which are located on locally over-steepened terrain at the upper parts of the catchments with gradient between 35° and 45°.

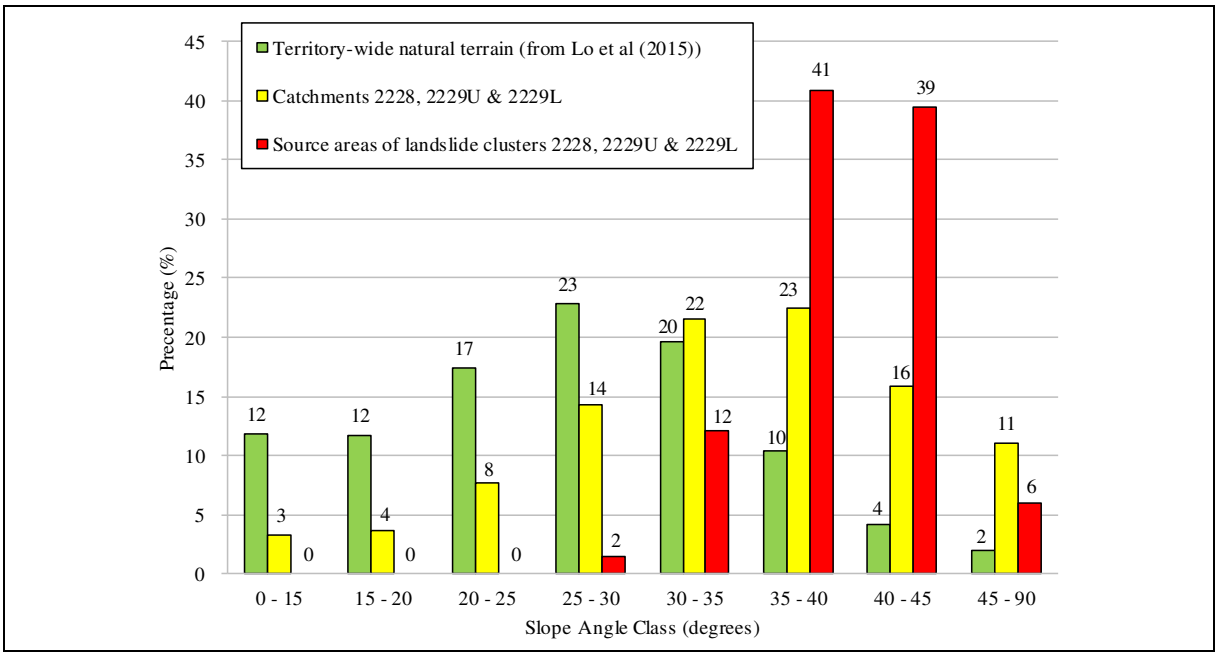

Figure 6.1 Slope Angle Distribution

The landslides were mostly originated from the interface of two distinct landforms along the nearly continuous steep terrain below the ridgelines at the upper part of the catchments. The rounded, shallow gradient ridgelines at the crest areas of the three catchments above the three landslide clusters forming the upper landform are generally older. This upper landform is covered with a mantle of colluvium overlying the in-situ weathered tuff. The terrain below prominent convex break-in-slopes forming the lower landform is relatively younger. The boundary between these two landforms delineated the erosion front where the terrain gradient sharply increases. Around this boundary, mass wasting process in the form of retrogressive failures occurs on the over-steepened areas particularly adjacent to heads of drainage lines and locations of past landslides, resulting in gradual upward migration of the erosion front towards the ridgelines (Figure 6.2). This is supported by the fact that about 75% and 70% of the source areas of the 2018 landslides are in close proximity to or overlapped with heads of drainage lines and past landslides respectively. The hillside retreat process remains active as evidenced by the nearly continuous steep erosion front with a high concentration of past landslides and head of drainage lines rendering these boundary areas particularly vulnerable to landsliding (Figure 6.3).

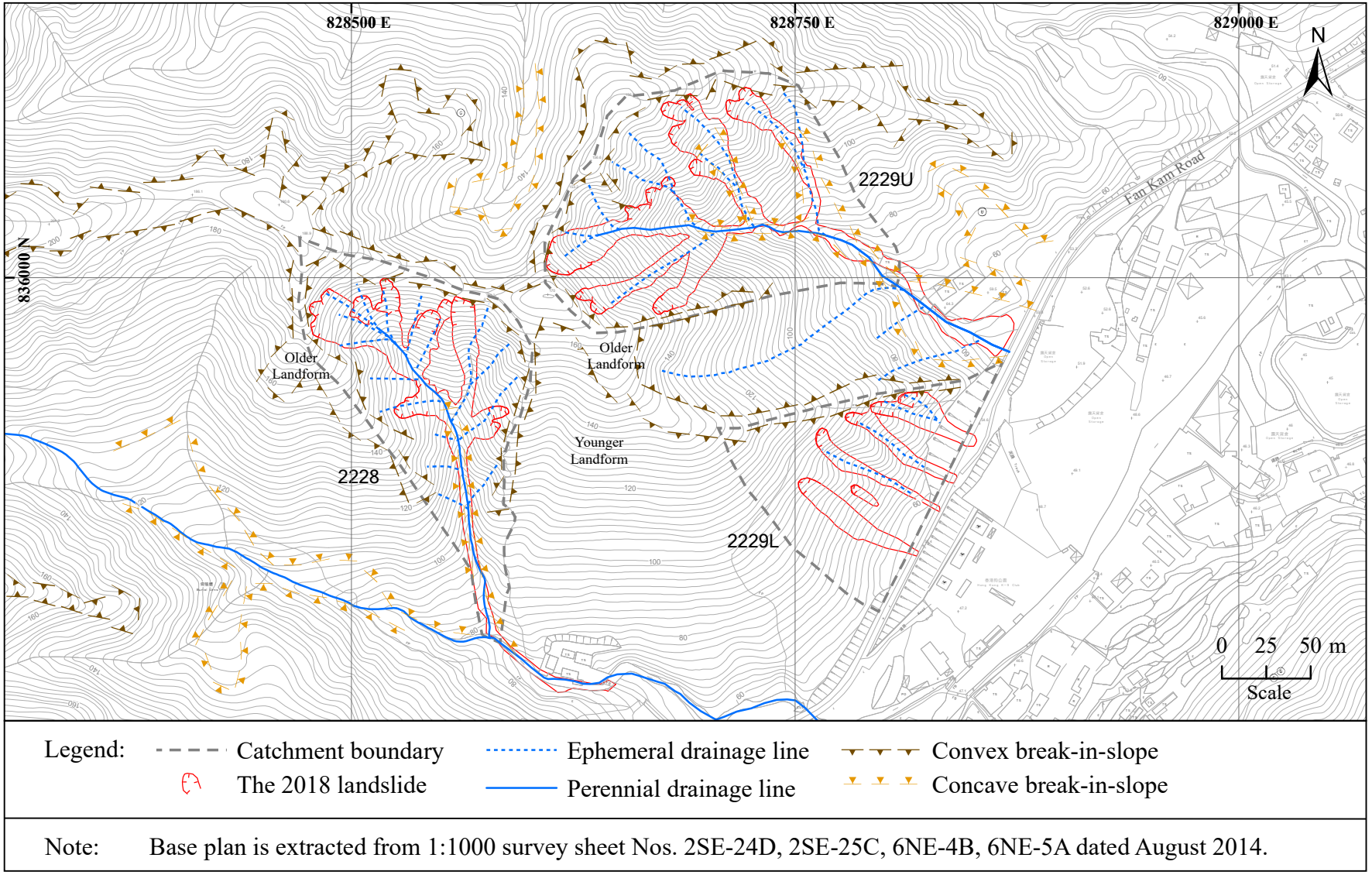

Figure 6.2 Geomorphological Setting

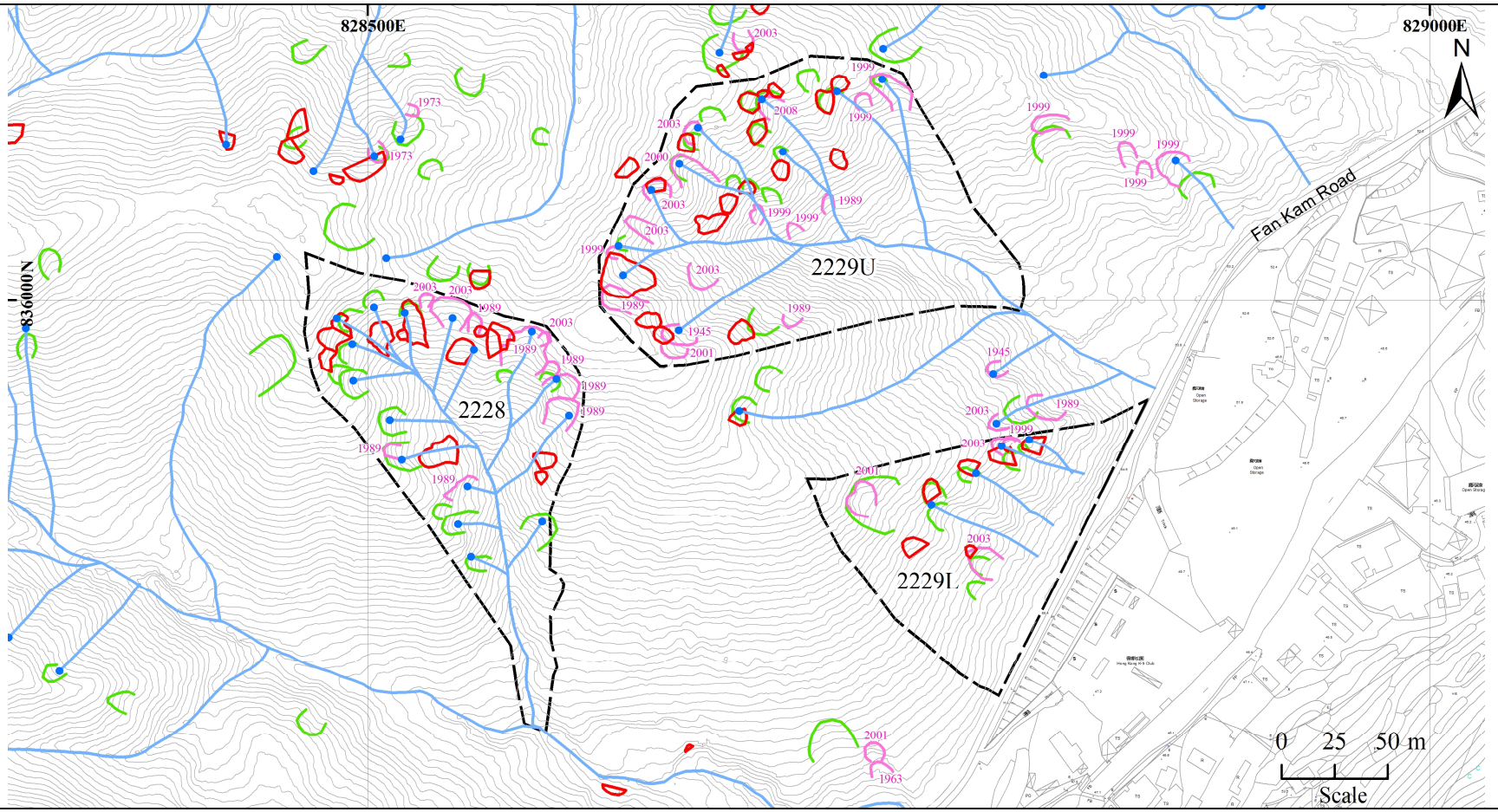

Legend:

2018 landslide source area	Catchment boundary	1999	Crown of recent landslide
Head of drainage line	Drainage line		Crown of relict landslide

Note: Contour lines are generated from LiDAR data collected in 2010.

Figure 6.3 Spatial Relationship of the 2018 landslides with Drainage Lines and Past Landslide Activities

Referring to Section 2.2, the northeast-trending regional Tai Lam Fault is located along Fan Kam Road, adjacent to the three catchments. As revealed by field mapping and a review of existing ground investigation records, the locations of the three landslide cluster areas proximate to Fan Kam Road aligned with the Tai Lam Fault appears to be coincident with a high intensity of persistent quartz veins (up to 200 mm wide) within the landslide source floors and debris trails. In addition, quartz fragments and blocks were observed on the landslide scarps, within the landslide debris and on the ground surface along the ridgeline (Figure 6.4). Some existing ground investigation records also identified quartz fragments in the colluvium in addition to quartz veins in the weathered tuff. The notable intensity of quartz in the insitu weathered materials as well as the superficial deposits may reflect a potentially higher degree of hydrothermal and metamorphic activities in association with the regional Tai Lam Fault along Fan Kam Road. Reference can be made to Sections 2.2 and 5 for other information pertaining to the site geology.

(a) Notable intensity of quartz veins traversing some of the landslide scars

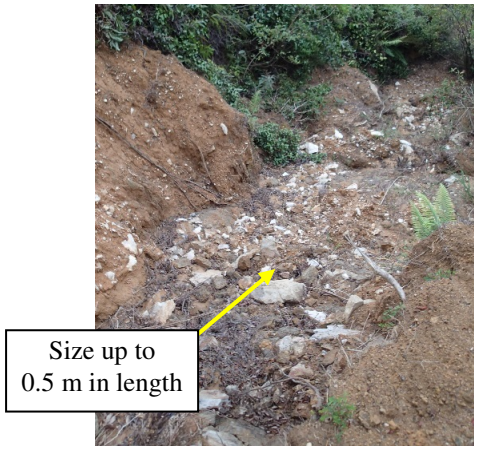

(b) Blocky quartz fragments within landslide debris along the debris trail

(c) Quartz veins within exposed soil along the debris trail

(d) Significant accumulations of quartz fragments on the ground surface (colluvial regolith) along the ridgeline of 2228 and 2229U

Figure 6.4 Quartz Veins and Quartz Fragments

7 Other Influence

7.1 Anthropogenic Activities

As revealed by API, there are several apparent excavation pits/trenches, considered to be mostly related to past military or mining activities, proximate to the three landslide clusters in particular on the ridgeline above landslide cluster 2229U (Figure 4.1). It is noted that only a few 2018 landslides are situated close to the pits/trenches. The other landslides are several ten metres away from the pits/trenches. With regard the present conditions, the pits/trenches (typically less than 1m in depth) are generally degraded with vegetation growth over time (Figure 7.1). While the edges of the pits/trenches may form oversteepened faces increasing the susceptibility to landsliding, none of the landslides were found to have encroached into any pits/trenches. The pits/trenches may have allowed ponding, promoting enhanced infiltration into the slope which in turn increase the susceptibility to landsliding. It is noted that only about 20% of the landslides are situated at the downslope areas of the pits/trenches. As such, no strong correlation can be deduced between anthropogenic activities and the 2018 landslides.

Figure 7.1 Conditions of Excavation Pits

7.2 Hillfire

The surface characteristics of hillside could be altered by hillfire in that it destroys vegetation (i.e. the surface protection) bringing an adverse effect on slope stability. On the other hand, hillfire could lead to water repellency in soil rendering reduced infiltration and increased surface runoff and erosion (Zheng & Lourenço, 2018). These effects are temporary in nature, generally prior to the re-establishment of vegetation. The hillfire records within the region over the past decade have been reviewed. The landslide cluster areas and their vicinity were not subjected to hillfire except for a zone to the west of landslide cluster 2228 where it exhibited hillfire in 2017 (Figure 4.1). Judging from the site setting, this hillfire zone would generally divert any runoff to the downslope area southwest of it, essentially having negligible effect on the three landslide cluster areas. Therefore, no particular correlation can be deduced between hillfire and the 2018 landslides.

8 Analysis of Rainfall Records

Rainfall data was obtained from the nearest automatic raingauge No. D42 managed by Drainage Services Department (DSD), which is located at the Fire Services Department Pat Heung Training School some 1 km to the southwest of the landslide site (Figure 1.1). The raingauge was established in 1998 and records rainfall data at 5-minute intervals. The daily rainfall recorded over the month preceding the landslides and the hourly rainfall recorded between 12:00 a.m. on 28 August 2018 and 2:00 p.m. on 30 August 2018 are presented in Figure 8.1.

An analysis of the return periods for various durations of rolling rainfall preceding the incidents recorded by DSD raingauge No. D42 has been carried out. While statistical parameters are not available for this raingauge, statistical parameters derived by Tang & Cheung (2011) for the nearest GEO raingauge No. N05 have been adopted for the analysis. Results of the analysis show that the rainfall duration of 2-hour was the most severe with a corresponding return period of about 900 years (Table 8.1). Other short-duration rainfalls for rainfall durations of 1-hour and 4-hour were also severe with estimated return periods of about 180 and 170 years respectively.

The maximum rolling rainfall preceding the incidents on 29 August 2018 has been compared with that of the previous major rainstorms as recorded by DSD raingauge No. D42 and the results are presented in Figure 8.2. The 29 August 2018 rainstorm was the most severe for almost all rainfall durations since the operation of the raingauge in 1998.

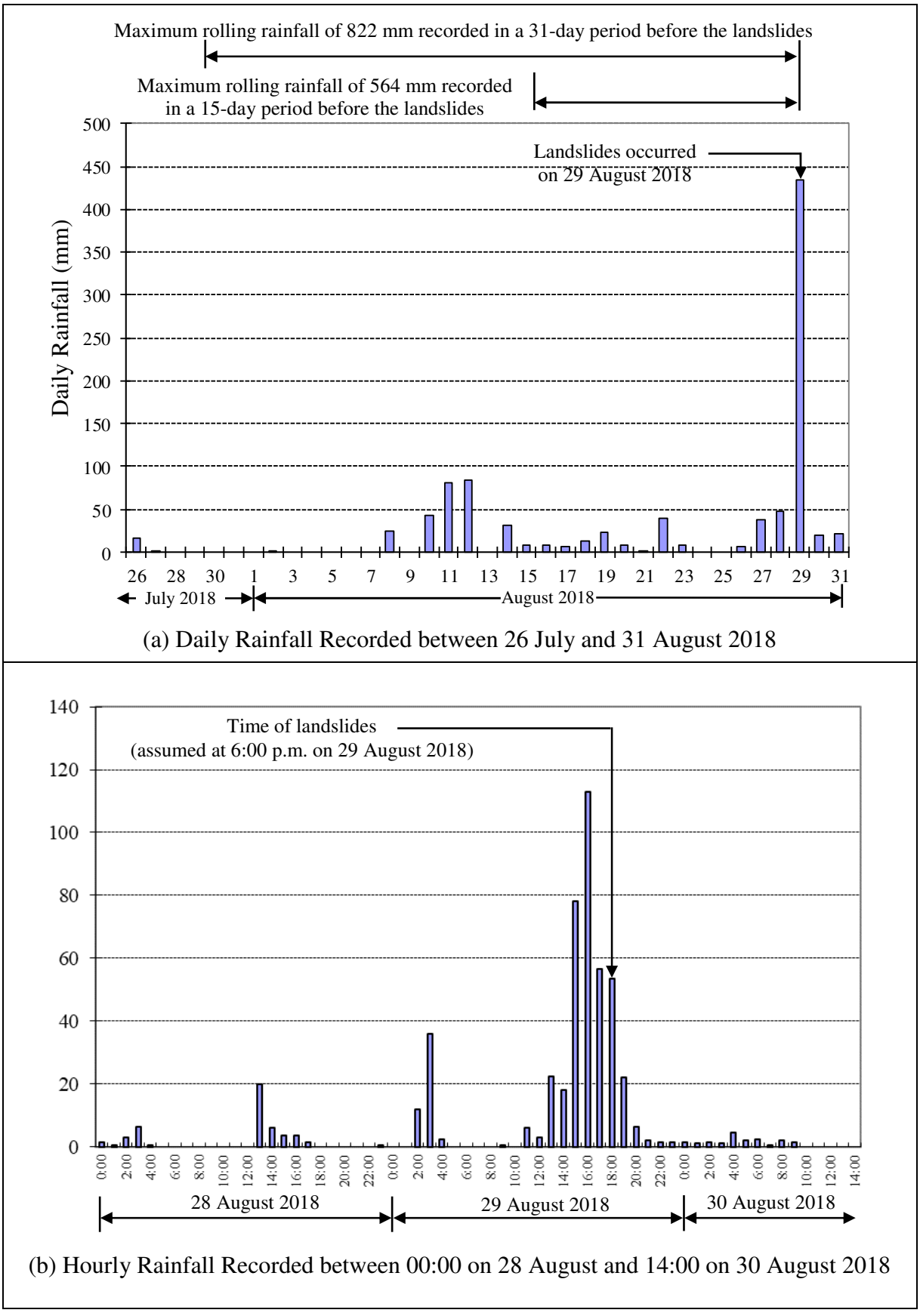

Figure 8.1 Daily and Hourly Rainfall Recorded at DSD Rainguage No. D42

Table 8.1 Maximum Rolling Rainfall at DSD Raingauge No. D42 for Selected Durations Preceding the Landslides and Estimated Return Periods

Duration	Maximum Rolling Rainfall (mm)	End of Period (Hours)	Estimated Return Period (Years) Note 4
5 Minutes	15	16:20 on 29 August 2018	8
15 Minutes	37	16:30 on 29 August 2018	9
30 Minutes	70	16:40 on 29 August 2018	38
1 Hour	121	16:40 on 29 August 2018	181
2 Hours	197.5	17:15 on 29 August 2018	896
4 Hours	265.5	17:30 on 29 August 2018	171
6 Hours	291	18:00 on 29 August 2018	82
8 Hours	297	18:00 on 29 August 2018	44
12 Hours	297.5	18:00 on 29 August 2018	24
24 Hours	348.5	18:00 on 29 August 2018	14
48 Hours	428	18:00 on 29 August 2018	14
4 Days	439.5	18:00 on 29 August 2018	6
7 Days	481.5	18:00 on 29 August 2018	5
15 Days	564	18:00 on 29 August 2018	4
31 Days	822	18:00 on 29 August 2018	4

Notes:
(1) Maximum rolling rainfall was calculated from 5-minute rainfall data provided by DSD.
(2) DSD raingauge No. D42 is located at Fire Services Department Pat Heung Training School about 1 km to the southwest of the landslide site.
(3) For the pupose of rainfall analysis, the time of the landslides was assumed to be at 6:00 p.m. on 29 August 2018.
(4) The return periods were estimated based on the method described by Tang & Cheung (2011) with reference to the statistical parameters from GEO raingauge No. N05 since 1983 which is the nearest GEO raingauge.

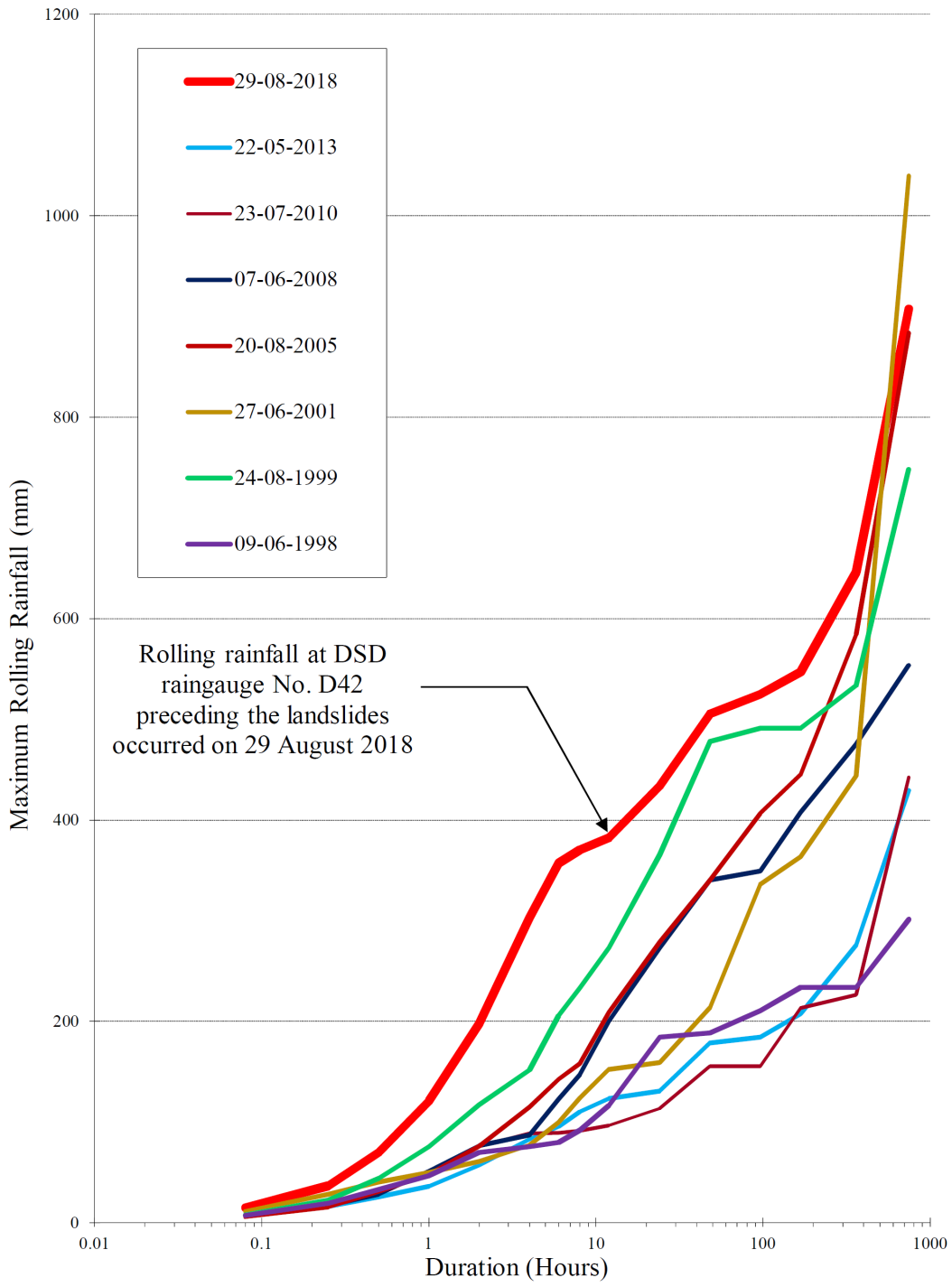

Notes:

(1) Rainfall data are evaluated from 5-minute readings from DSD raingauge No. D42 (located at Pat Heung FSD Training School in Fanling about 1 km to the southwest of the landslide site).

(2) Raingauge No. D42 started its operation since 1998 and the maximum rolling rainfalls are estimated from rainstorms afterwards.

Figure 8.2 Maximum Rolling Rainfall Preceding the Landslides and Selected Previous Major Rainstorms Recorded at DSD Raingauge No. D42

9 Debris Mobility

The debris from the source areas entered the central main drainage lines of catchments 2228 and 2229U where the debris became confined and channelised before coming to rest at the relatively gentle terrain just before reaching Fan Kam Road. The total travel distance of both channelised debris flows was about 300 m (excluding the outwash) of which about 80 m and 160 m of the lowest segment of the debris trails of landslide cluster 2228 and 2229U respectively have an overall gradient of 15° or less. The travel angle measuring from the crown of uppermost source area to the end of debris trails are about 20° in both cases. The channelised debris flows appear fairly mobile based on a comparison with previous events of a similar scale in Hong Kong (Figures 9.1 and 9.2).

Theoretical analysis of the debris mobility of the channelised debris flows associated with landslide clusters 2228 and 2229U have been carried out using DAN-W (Release 10). The topography adopted for the modelling is based on terrain profile obtained from the pre-failure territory-wide air-borne LiDAR survey. The thickness of the displaced materials within the source areas is estimated from a comparison of the pre- and post-failure topography together with field measurements. A Voellmy rheological model is adopted in the analyses and, for simplicity, it has been assumed that all the materials in the source areas displaced simultaneously. Since the landslide clusters consist of multiple source areas and contributing debris from both flanks of the incised drainage lines, it has been assumed that debris from the flanks was entrained along the debris flow path and the entrainment volume is adjusted to reasonably fit the mass balance of the landslides as shown in Figures 5.3 and 5.4.

The results of the analyses show that a turbulence coefficient of 500 m/s^2 and a base friction angle of about 11° for the whole debris trail gave a best fit to the observed debris runout for both landslide clusters 2228 and 2229U. The results are consistent with the recommended parameters for debris mobility modelling using the Voellmy model for channelised debris flows in Hong Kong that are not deemed to be prone to watery debris flows due to an adverse site setting such as along a major drainage line with a large catchment (e.g. >100,000 m^2) or many tributaries (GEO, 2011).

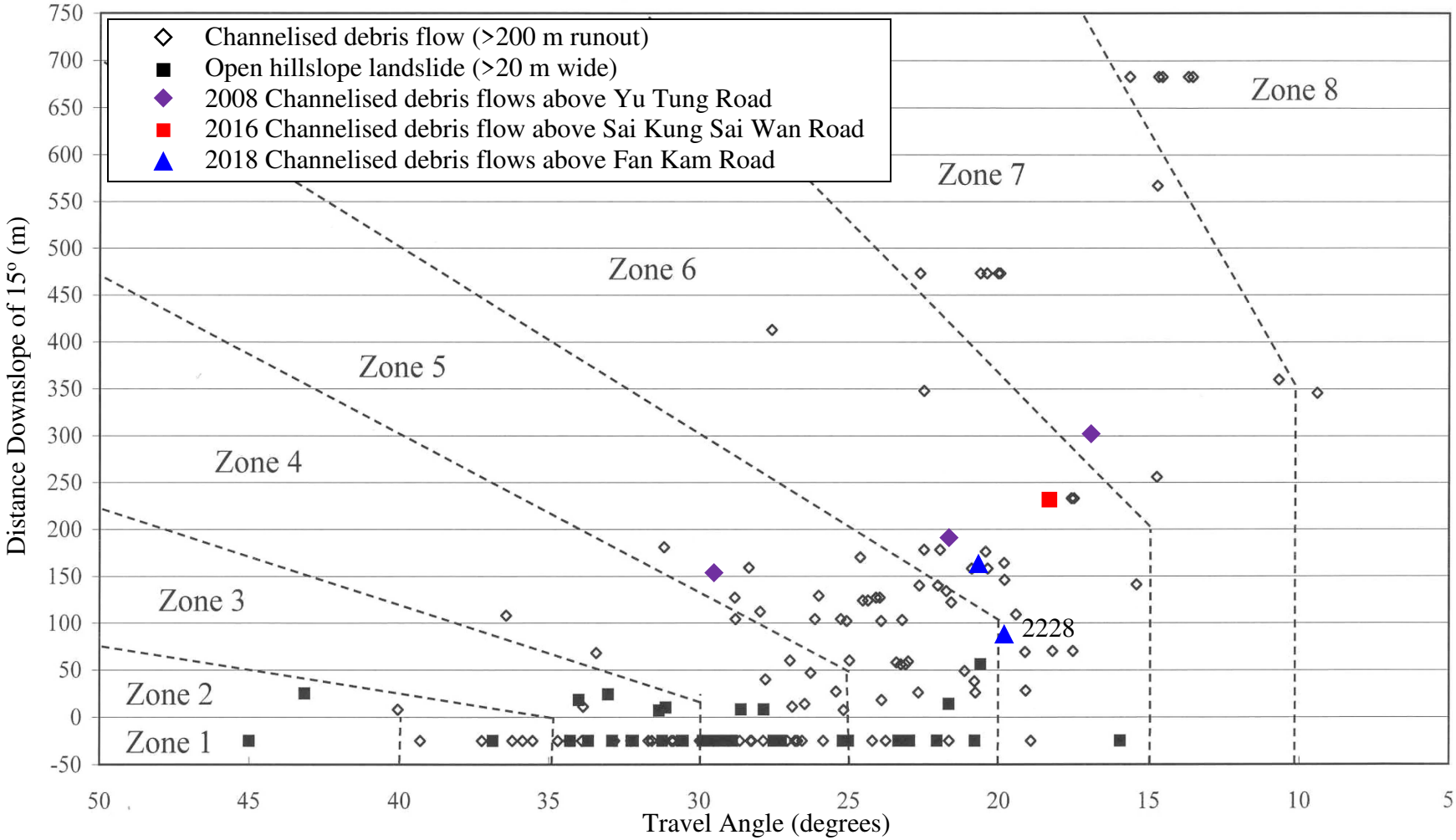

Note: Original chart extracted from Wong et al (2006).

Figure 9.1 Proximity Zones and Debris Runout Data from the 2018 Landslides

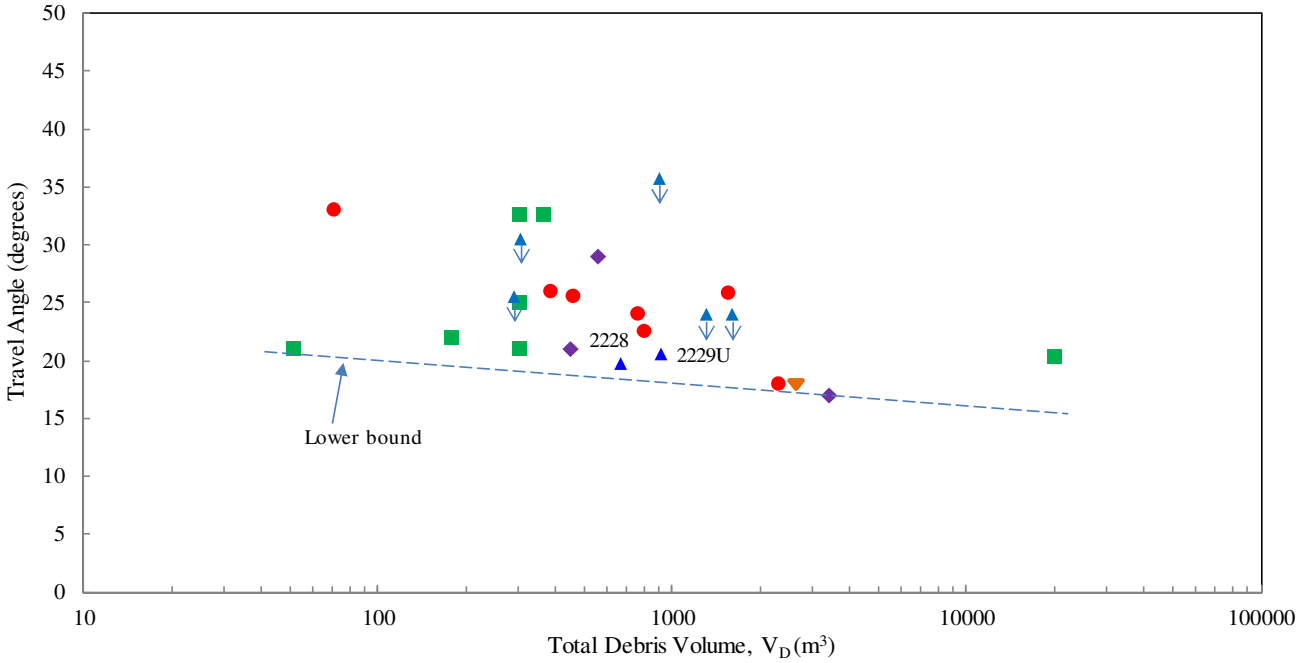

Legend:

Channelised debris flows:

- Wong et al (1998) (upper bound)
- Relevant data based on Franks (1998)
- Data extracted from landslide study reports and values are reported in Hungr (1998) and Ayotte & Hungr (1998)
- 2008 natural terrain landslides above Yu Tung Road
- 2016 natural terrain landslide above Sai Kung Sai Wan Road
- 2018 natural terrain landslides above Fan Kam Road

Note: Total debris volume is taken as the summation of source volume and erosion volume along the debris trail.

Figure 9.2 Data on Debris Mobility for Channelised Debris Flows of Different Scale in Hong Kong

10 Discussion

10.1 Probable Mechanism and Causes of the Landslides

The close correlation between the landslides and the intense rainstorm suggests that the failures were rain-induced. The landslides, which appeared in three separate clusters, were generally originated from the locally over-steepened terrain with gradient between 35° and 45° below prominent convex break-in-slopes near the upper part of the respective catchments. Such areas represent the interface of two distinct landforms where the hillside retreat process remains active, as evidenced by the nearly continuous steep erosion front with a high concentration of past landslides and heads of drainage lines. Associated with the on-going geomorphological process, the steep terrain in this locality has predisposed it to the risk of landsliding. It is noted that the source areas of most of the 2018 landslides overlapped with or were close to the locations of past landslides where reactivation or retrogression of previous failures could have contributed to the present failures.

The landslides typically involved shallow detachment (generally less than 1 m in depth) of the thin mantle of colluvium overlying the in-situ weathered materials. The failures are likely to have been caused by infiltration rendering the development of perched water table within the colluvium above the strata boundary with a permeability contrast. The close proximity of the regional Tai Lam Fault along the alignment of Fan Kam Road could have an implication on landslide susceptibility of the areas. The persistent quartz veins observed in the exposed weathered materials could also have impeded the groundwater flow exacerbating the build-up of the perched water and hence contributed to the failures.

Anthropogenic activities could have played a role in a small fraction of the landslides where some degraded trenches/pits were located in their upslope areas that might have promoted enhanced infiltration in the event of ponding. Past hillfire records have been reviewed which indicate that hillfire has minimal effect on the landslides.

10.2 Probable Causes of the Landslide Clustering

Under an intense rainstorm, numerous landslides may occur on a hillside particularly in the susceptible areas. These landslides may develop into landslide clusters if the susceptible areas are closely spaced or connected. Notably, many 2018 landslides on the hillside above Fan Kam Road occurred in close proximity or with the scars/trails merged in some cases forming three distinct landslide clusters. A site-specific assessment has been conducted with a view to identifying the factors concerning landslide susceptibility of the subject hillside that could have caused landslide clustering. Details of the assessment are presented in Appendix C.

The findings of the assessment suggest that the development of landslide clustering over the hillside above Fan Kam Road is the result of a complex combination of interconnected factors controlling landslide susceptibility. The continuous steep terrain has evolved from an active geomorphological process, particularly for those areas over-steepened by the development of heads of drainage lines and past landslides. There also appears to be a tendency of landslide cluster to develop around the heads of drainage lines. The steep

gradient coupling with the high density of heads of drainage lines promoted erosion and further instability and could have been a prominent predisposing factor to landslide clustering.

In addition, the adverse geological settings are considered to be the other factors contributing to the landslide clustering. This involves the presence of regolith susceptible to landslide initiation, viz. colluvium being weaker and more vulnerable to infiltration as compared with in-situ weathered materials. Besides, areas in close proximity to the regional Tai Lam Fault along Fan Kam Road may have a higher susceptibility to landslide clustering. Associated with the regional fault, there could be a higher degree of hydrothermal and metamorphic activities. With the fractured nature of the fault and influence of the activities associated with faulting, materials lying within the fault zones and their close proximity are typically relatively weaker. The relatively weaker materials together with the potential adverse effect on the groundwater regime associated with the notable intensity of persistent quartz veins in the insitu weathered materials could have contributed to the landslide clustering. Such influence appears to have been manifested by the observed trend of having a significantly higher density of 2018 landslides and past landslides closer to Fan Kam Road.

11 Conclusions

The landslides occurring on the hillside above Fan Kam Road on 29 August 2018 developed into three distinct clusters of multiple failures. The landslides were triggered by an intense rainstorm which was the most severe since records began in 1998. The failures were probably induced by infiltration through shallow colluvium regolith causing the development of a perched water table above the interface between colluvium and underlying weathered tuff. The open hillslope failures from landslide cluster 2229L were generally small and not mobile with landslide debris deposited locally on Fan Kam Road. Landslide clusters 2228 and 2229U within topographic depressions developed into fairly mobile channelised debris flows with runout distance of about 300 m excluding the outwash. Landslide debris from these two landslide clusters mostly came to rest before reaching Fan Kam Road but subsequent outwash brought further debris onto the road, resulting in traffic disruption among other consequences.

The landslides on the hillside are characterised by high landslide density and strong clustering in the volcanic terrain. They generally occurred within the steep colluvial terrain and mostly clustered around heads of drainage lines and/or past landslides. The complex combination of the interconnected geomorphological and geological factors is conducive to the high landslide activity of the catchments and susceptibility to multiple failures under heavy rainfall.

12 References

Ayotte, D & Hungr O. (1998). *Runout Analysis on Debris Flows and Debris Avalanches in Hong Kong*. Geotechnical Control Office, Hong Kong, 90 p.

Franks, C.A.M. (1998). *Study of Rainfall Induced Landslides on Natural Slopes in the Vicinity of Tung Chung New Town, Lantau Island (GEO Report No. 57).* Geotechnical Control Office, Hong Kong.

Geotechnical Control Office (1988). *Yuen Long: Solid and Superficial Geology, Hong Kong Geological Survey, Map Series HGM 20, Sheet 6, 1:20,000 scale.* Geotechnical Control Office, Hong Kong.

Geotechnical Control Office (1989). *San Tin: Solid and Superficial Geology, Hong Kong Geological Survey, Map Series HGM 20, Sheet 2, 1:20,000 scale.* Geotechnical Control Office, Hong Kong.

Geotechnical Engineering Office (2011). *Guidelines on the Assessment of Debris Mobility for Channelized Debris Flows (GEO Technical Guidance Note 29).* Geotechnical Engineering Office, Hong Kong, 6 p.

Hungr, O. (1998). *Mobility of Landslide Debris in Hong Kong: Pilot Back Analyses Using a Numerical Model.* Geotechnical Engineering Office, Hong Kong, 50 p.

Lo, F.L.C., Law, R.P.H. & Ko, F.W.Y. (2015). *Territory-wide Rainfall-based Landslide Susceptibility Analysis (Special Project Report No. SPR 1/2015).* Geotechnical Engineering Office, Hong Kong, 27 p.

Scott Wilson (Hong Kong) Ltd. (1999). *Specialist API Services for the Natural Terrain Landslide Study - Task B Final Report.* Report to Geotechnical Engineering Office, Hong Kong, 9 p. plus 4 maps.

Sewell, R.J., Campbell, S.D.G., Fletcher, C.J.N., Lai, K.W. & Kirk, P.A. (2000). *The Pre-Quaternary Geology of Hong Kong.* Geotechnical Engineering Office, Hong Kong, 181 p. plus 4 maps.

Tang, C.S.C. & Cheung, S.P.Y. (2011). *Frequency Analysis of Extreme Rainfall Values (GEO Report No. 261).* Geotechnical Engineering Office, Hong Kong, 209 p.

Wong, H.N., Lam, K.C. & Ho, K.K.S. (1998). *Diagnostic Report on the November 1993 Natural Terrain Landslides on Lantau Island (GEO Report No. 69).* Geotechnical Engineering Office, Hong Kong, 98 p.

Wong, H.N., Ko, F.W.Y. & Hui, T.H.H. (2006). *Assessment of Landslide Risk of Natural Hillsides in Hong Kong (GEO Report No. 191).* Geotechnical Engineering Office, Hong Kong, 117 p.

Zheng, S. & Lourenço, S.D.N. (2018). *Post-wildfire debris flows in Greater China. 2nd JTC1 Workshop on Triggering and Propagation of Raid Flow-like Landslides.* Hong Kong.

Appendix A

Aerial Photograph Interpretation

Contents

List of Tables

List of Figures

A.1 Introduction

An aerial photograph interpretation (API) has been carried out as part of the desk study for the purposes of establishing the site history, past instability and geomorphological characteristics of the site. A review of available aerial photographs taken between 1945 and 2017 was undertaken (see list in Table A1). Based primarily on the 1963 aerial photographs, with some additional observations from other relevant aerial photographs, observations relating to the site history and past instability are shown on Figures 4.1 to 4.3, with the morphology and hydrology shown in Figure 6.2. Pertinent observations from the API are summarised in Figures A1 and A2.

A.2 Summary

The site is located in natural terrain catchments within the Lam Tsuen Country Park to the northwest of Fan Kam Road. The catchments for which the three landslide clusters developed, denoted as catchments 2228, 2229U and 2229L, are located at the lower portion of a spur descending from the summit of Kai Kung Leng. These three catchments are delineated by well-defined ridgelines, with heads of the catchments located immediately below it. Extending downslope from the ridgelines is a series of spurlines that form the catchments boundaries. The terrain immediately downslope from the ridgelines is typically steep with slope gradient between 35° and 45° while the terrain further downslope is of shallower gradient.

Catchments 2228 and 2229U contain south- to southeast-trending incised central main drainage lines which are fed by several ephemeral drainage lines on the valley flanks. All of these drainage lines drain down to Fan Kam Road and eventually confluent into Sheung Yue River.

Numerous landslides, including relict landslides (RL1 to RL37) and recent landslides (LS1 to LS30) can be identified in the three catchments. These landslides are generally observed as shallow, rounded, degraded depressions predominately located at the head of drainage lines or near the ridgelines.

The main anthropogenic activities observed in the vicinity is the construction of Fan Kam Road and associated slope formation, at the toe of the hillside, which was completed in 1954. Trenches/pits excavation related to military or mining activities are apparent along ridgelines and spurs since 1954, mainly at the northern portion of catchment 2229U along the ridgeline. Dwellings at the outlets of catchments 2228 and 2229U were constructed between 1963 and 1972.

Catchments 2228, 2229U and 2229L and their vicinity have been frequently affected by hillfire. Hillfire events in 1973, 1975, 1981, 1993, 2003 and 2017 are identified. Predominantly the upper portions of catchments 2228 and 2229U were affected.

A.3 Detailed Observations

This appendix sets out the detailed observations made from an interpretation of aerial photographs taken between 1945 and 2017. A list of the aerial photographs studied is presented in Table A1 and a location plan is shown in Figure A1.

Year	Observations
1945	Poor resolution, high-flight photographs preclude detailed interpretation. The site is located in natural terrain catchments within the Lam Tsuen Country Park to the northwest of Fan Kam Road. The catchments for which the three landslide clusters developed (i.e. catchments 2228, 2229U and 2229L) are located at the lower portion of a spur descending from the summit of Kai Kung Leng. These three catchments are delineated by well-defined ridgelines, with heads of the catchments located immediately below. Extending downslope from the ridgelines is a series of spurlines that form the catchment boundaries. The three catchments are generally lightly vegetated with grass and shrubs, relative dense vegetation can be observed along the central main drainage lines, while some patches of highly reflective bare earth surface can be observed at the ridgelines, which probably patches of surface erosion or anthropogenic disturbance. The toe of the hillside consists of agricultural terraces on the alluvial plain at both sides of Sheung Yue River. Fan Kam Road and the associated man-made slopes have not yet been formed. Recent landslide LS1 is observed at the southern portion of catchment 2229U. It is located near the head of drainage line below the ridgeline.
1954	Poor resolution, high-flight photographs preclude detailed interpretation. Photolineaments trending NW-SE and NE-SW are visible. Fan Kam Road and the associated man-made slopes have been formed along the toe of the hillside. Newly appeared highly reflective areas can be observed at the lower portion of catchment 2229U, which connected to Fan Kam Road and likely to be anthropogenic disturbance.

Year	Observations
1963	These photographs are of excellent resolution and the terrain morphology is much clearer. A number of relict landslides (RL1 to RL37) can be identified within the three catchments (i.e. 14 in catchment 2228, 15 in catchment 2229U and eight in catchment 2229L). Among those identified relict landslides, one of them has a sharp scarp (Class A), 14 of them have rounded scarps (Class B) and 22 of them are shallow depressions with gentle break-in-slopes (Class C). These relict landslide features are predominately located at the heads of drainage lines or near the ridgelines. Most of these landslides are shallow in nature and have been vegetated with grass. Recent landslide LS1 observed in 1945 is likely to have been considered as relict landslide feature in ENTLI with tag No. 06NEB0212E as the shallow landslide scar has been overgrown with vegetation and appeared as a depression under shadow in the aerial photographs. The three catchments and their vicinity are generally underlain by volcanic saprolite, possibly blanketed with a thin veneer of colluvium below a prominent convex break-in-slope. Valley colluvium is commonly present along the central main drainage lines of catchments 2228 and 2229U. Relict or recent landslide debris can be discerned at downslope of some of the relict or recent landslides. Photolineaments trending NE-SW and NW-SE can be observed, which are probably associated with geological structures (e.g. faults or joints). Some of the lineaments are sub-parallel to each other, which possibly reflecting the dominant joint set orientation. Several squatters (H1 to H3) with access road connecting to Fan Kam Road can be discerned at the toe of catchment 2228, while squatters H4 to H6 can be discerned to the northeast of catchment 2229U. Agricultural activities (A1 to A3) can also be discerned in the vicinity. Trenches/pits excavation related to military or mining activities, are clearly observed and predominantly distributed along the ridgelines and spurs adjacent to catchments 2228 and 2229U. Some bands of darker tone lineaments can be observed, which generally surround the trenches/pits excavation and may be related to fencing for the military features.
1964	No significant changes.
1972	Site formation works (M1 and M2) and construction of low-rise structures (H7 to H10) can be discerned at the toe of catchments 2228 and 2229U.

Year	Observations
1973	Small structure H3 at the toe of catchment 2228 appears to be demolished and slope No. 6NE-B/C36 has been formed. The upper northern flank of catchment 2229U appears to have been affected by hillfire event HF2.
1974	No significant changes.
1975	The northern flank of catchment 2229U appears to have been affected by hillfire event HF4. Besides, the vegetation density of catchment 2229L reduced and highly reflective soil surface can be observed through the sparse vegetation.
1976	No significant changes.
1978	No significant changes.
1979	No significant changes.
1981	The northern flank of catchment 2229U has been affected by hillfire event HF8.
1982	Electricity poles have been erected from the northern flank of catchment 2229U to the lower portion of catchment 2228.
1983	No significant changes.
1985	No significant changes.
1986	No significant changes.
1987	No significant changes.
1988	No significant changes.

Year	Observations
1989	Seven recent landslides (LS2 to LS8) can be discerned within catchment 2228. Landslides LS2, LS3 and LS4 (ENTLI Nos. 06NEB1983E, 06NEB1982E & 06NEB1979E) located at the upper portion of catchment 2228 are isolated landslides with an estimated source volume of about 30 m^3. Their debris primarily deposited at the toe of the source areas. Landslides LS5 to LS8 (ENTLI Nos. 06NEB1980E, 06NEB2088E, 06NEB1981E and 06NEB2089E) forming a landslide cluster at the eastern flank of catchment 2228 with a total estimated source volume of about 530 m^3 converged into drainage line and turned into channelized debris flows. The debris trail can be traced to the toe of catchment at the drainage line with a runout distance of about 200 m. Landslide LS3 and two adjoining landslides LS6 & LS7 coincide with the locations of relict landslides RL8 and RL2 respectively. Three recent landslides (LS9 to LS11) are identified within catchment 2229U. Landslides LS9 and LS10 are corresponding to ENTLI Nos. 06NEB2081E and 06NEB1978E while landslide LS11 was not recorded in ENTLI. All of them are isolated landslides with their debris primarily deposited at the toe of the source areas. Low-rise structures H9 and H10 appears to have been abandoned and the platform M2 has been over-grown with vegetation.
1990	No significant changes.
1991	No significant changes.
1992	Small structure H11 has been constructed to the east of squatter H2.
1993	Upper portion of catchment 2228 has been affected by hillfire event HF10. Excavation (M6) can be observed at the lower northern flank of catchment 2229U which possibly associated with anthropogenic disturbance. Damages of the roof of squatter H7 at the lower portion of catchment 2229U can be observed and the squatter appears to have been abandoned.
1994	No significant changes.
1995	Vegetation clearance can be observed at platform M1 in front of the squatter H7. Excavation appears to have been extended further upslope (M6a).
1996	The previous area of vegetation clearance at platform M1 appears to have been paved.
1997	No significant changes.

Year	Observations
1998	No significant changes.
1999	Recent landslide LS12 (ENTLI No. 06NEB2133E) are visible to be located at the northern portion of catchment 2229L. The debris appears to reach the crest of man-made slope No. 6NE-B/C12 without affecting Fan Kam Road. Five recent landslides (LS13 to LS17) have been identified within catchment 2229U. Landslides LS13, LS16 and LS17 (ENTLI Nos. 02SED0871E, 02SED0872E and 02SED0860E) are located at the heads of drainage lines of catchment 2229U whereas Landslide LS17 coincides with the location of relict landslide RL29. Landslides LS14 and LS15, which were not recorded in ENTLI, are located at the valley flank. The debris of these five landslides are primarily deposited just below the source areas. The roof of squatter H7 at the lower portion of catchment 2229U appears to have collapsed.
2000	Recent landslide LS18 (ENTLI No. 02SED0909E) has been identified within catchment 2229U, which is located at the upper portion near the head of drainage line. Its debris trail can be traced along the central main drainage line to about 45 m from squatter H8.
2001	Two recent landslides (LS19 and LS20) are visible within catchments 2229U and 2229L respectively. Landslide LS20 (ENTLI No. 06NEB2200E) coincides with the location of relict landslide RL30. The roof of H7 at the lower portion of catchment 2229U appears to have repaired.
2002	No significant changes.

Year	Observations
2003	Recent landslides LS21 to LS23 are identified near the crest of catchment 2228, which Landslide LS22 corresponds to ENTLI No. 06NEB2217E and landslides LS21 and LS23 were not recorded in ENTLI. Landslide LS23 is considered as a minor reactivation of recent landslide LS5. Four recent landslides (LS24 to LS27) are located at the upper portion of catchment 2229U. Landslides LS24, L25 and LS26 (ENTLI Nos. 02SED0905E, 02SED0894E and 02SED0895E) with a total source volume of about 220 m^3 converged into drainage line and turned into channelized debris flows. The debris trail can be observed just before reaching structure H8 at the toe of the catchment. The debris runout is about 180 m. Landslide LS27 (ENTLI No. 02SED0893E) coincides with the location of relict landslide RL24. Recent landslides LS28 and LS29 (ENTLI Nos. 06NEB2220E and 06NEB2219E) are located within catchment 2229L and the landslide debris do not reach Fan Kam Road. Landslide LS29 coincides with the location of relict landslide RL33. The upper portions of catchments 2228 and 2229U have been affected by a hillfire event HF12.
2004	No significant changes.
2005	Low-rise structure H12 have been constructed at the south of H2 and H11. The access road to the low-rise structures at the toe of catchment 2228 has been widened and paved.
2006	Structure H8 at the lower portion of catchment 2229U appears to have been abandoned, where the roof has been damaged. Over-grown of vegetation can be observed in the vicinity of H8.
2007	A new structure (H13) has been constructed adjacent to H12 at the toe of catchment 2228.
2008	Recent landslide LS30 (ENTLI No. 02SED0931E) is identified at the upper portion of catchment 2229U. It is located at the head of drainage line which coincides with the location of relict landslide RL20.
2009	A new structure (H14) has been constructed adjacent to H1 at the toe of catchment 2228.
2010	No significant changes.
2011	No significant changes.
2012	A new structure is visible at the previous location of squatter H7 at the toe of catchment 2229U.

Year	Observations
2013	No significant changes.
2014	No significant changes.
2015	No significant changes.
2016	No significant changes.
2017	The upper western portion of catchment 2228 appears to have been affected by hillfire event HF17.

Table A1 List of Aerial Photographs (Sheet 1 of 3)

Date taken	Altitude (ft)	Photograph Number
6 November 1945	20000	Y00823-25
17 November 1954	29200	Y02824-26
6 February 1963	3900	Y09649-52, Y09705-08
13 December 1964	12500	Y13039-40
14 December 1964	12500	Y13091-92
29 November 1972	3000	2562-64
20 December 1973	12500	7913-14
28 February 1974	12500	8231-31
21 November 1974	12500	9869-70
24 December 1975	12500	11936-37
23 November 1976	12500	16449-50
6 January 1978	12500	20641-42
30 October 1978	4000	22889
15 December 1978	12500	24504-05
7 November 1979	10000	27800-01
29 November 1979	10000	28275-76
13 January 1981	10000	35610-11
13 January 1981	10000	35620-21
20 September 1982	4000	43951-55
10 October 1982	10000	44682-83
22 December 1983	10000	52284-86
1 October 1985	10000	67363-64
3 August 1986	4000	A5631-34
5 January 1987	20000	A8457-58
10 June 1987	4000	A9444-45
16 January 1988	10000	A11934-35
2 June 1988	4000	A13044-45
13 November 1989	10000	A19191-92

Note: All aerial photographs are in black and white except for those prefixed with A, CN, CS, CW or E.

Table A1 List of Aerial Photographs (Sheet 2 of 3)

Date taken	Altitude (ft)	Photograph Number
3 December 1990	10000	A24257-58
29 October 1991	10000	A28705-06
11 November 1992	10000	A32929-30
2November 1993	3000	CN5125-27
9 November 1993	4000	A36503-05
19 May 1994	4000	A38345-47
19 December 1995	3500	CN13011-13
9 November 1996	10000	CN15944-45
25 October 1997	3000	CN18022-26
10 July 1998	3000	CN19946-47, CN20196-99
9 February 1999	3500	CN22473-76
5 November 1999	3500	CN24471-75
1 June 2000	3500	CN26469-72
20 September 2001	4000	CW32987-89
8 October 2002	8000	CW44606-08
1 June 2003	4000	CW48124-25
27 November 2003	3500	CW54052-54
5 March 2004	4000	CW56423-26
11 June 2004	2500	CW57812-14
3 April 2005	2500	CW64423-26
25 October 2005	4000	CW66512-14
22 December 2006	6000	CS03436-40
25 July 2007	3000	CW77484-85, CW77531-34
15 November 2007	8000	CW78743-44
28 February 2008	6000	CS10536-40
13 November 2008	6000	CS17789-91
24 November 2009	6000	CS26312-16
9 November 2010	8000	CW88115-16

Note: All aerial photographs are in black and white except for those prefixed with A, CN, CS, CW or E.

Table A1 List of Aerial Photographs (Sheet 3 of 3)

Date taken	Altitude (ft)	Photograph Number
9 November 2010	8000	CW88115-16
5 July 2011	6000	CS33269-74, CS33355-59
18 September 2012	6000	CS38504-06
21 June 2013	6000	CS43093-96, CS43148-52
13 April 2014	6000	CS52232-36, CS52293-98
13 April 2015	6000	CS58255-57
19 September 2016	6000	E002138-40C
4 April 2017	2500	E019669-76C, E019928-31C

Note: All aerial photographs are in black and white except for those prefixed with A, CN, CS, CW or E.

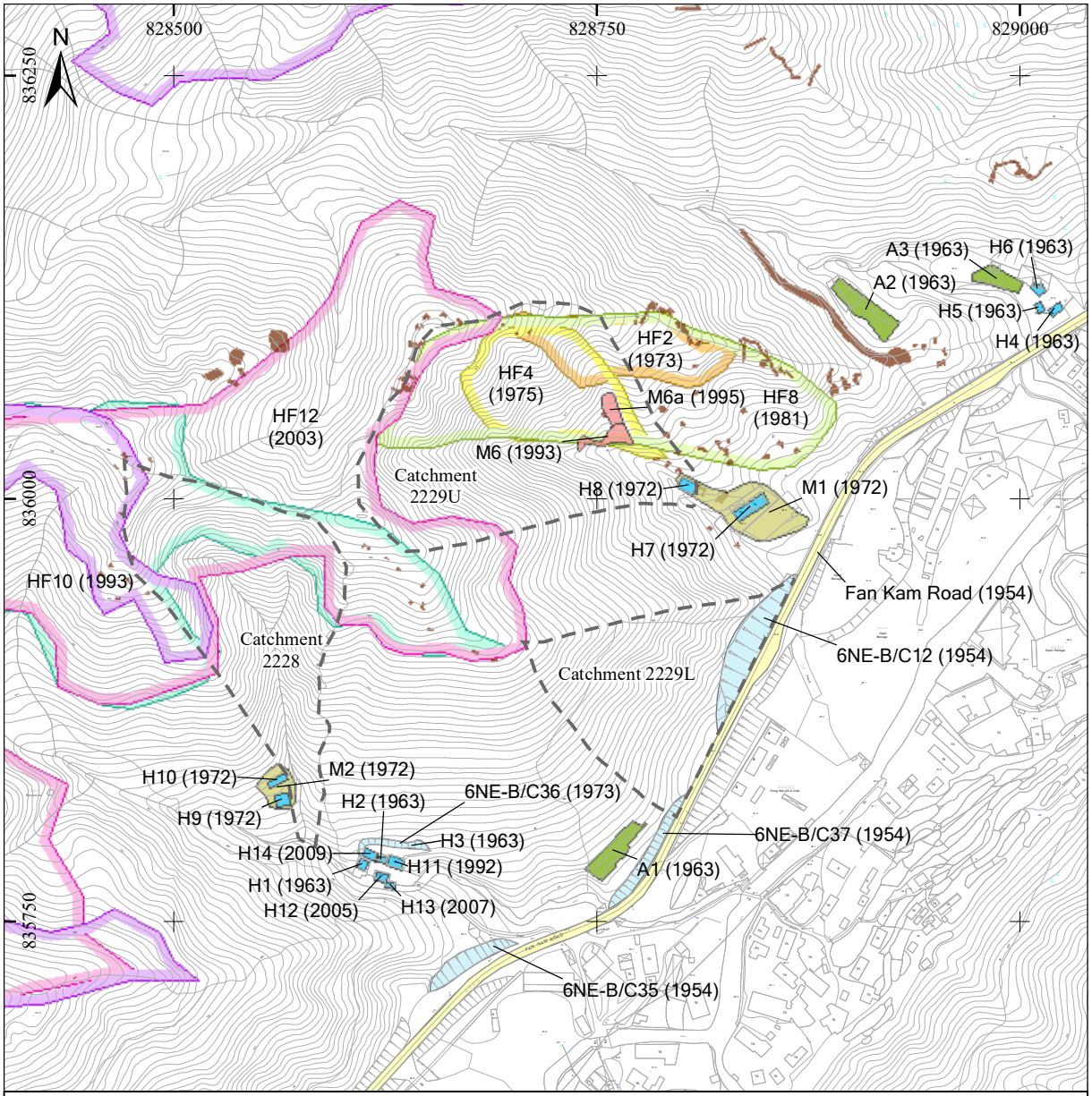

Legend:

- Catchment boundary
- Cut slope feature

Anthropogenic activities

- Agricultural land (A1 to A3)
- Low-rise structure (H1 to H14)
- Site formation (M1, M2)
- Excavation (M6, M6a)
- Fan Kam Road
- Inferred excavation and disturbance

Approx. extend of hillfire affected area

- HF2 (1973)
- HF4 (1975)
- HF8 (1981)
- HF10 (1993)
- HF12 (2003)
- HF17 (2017)

Note: Base plan is extracted from 1:1000 survey sheet Nos. 2SE-24D, 2SE-25C, 6NE-4B and 6NE-5A dated August 2014.

Figure A1 Site History

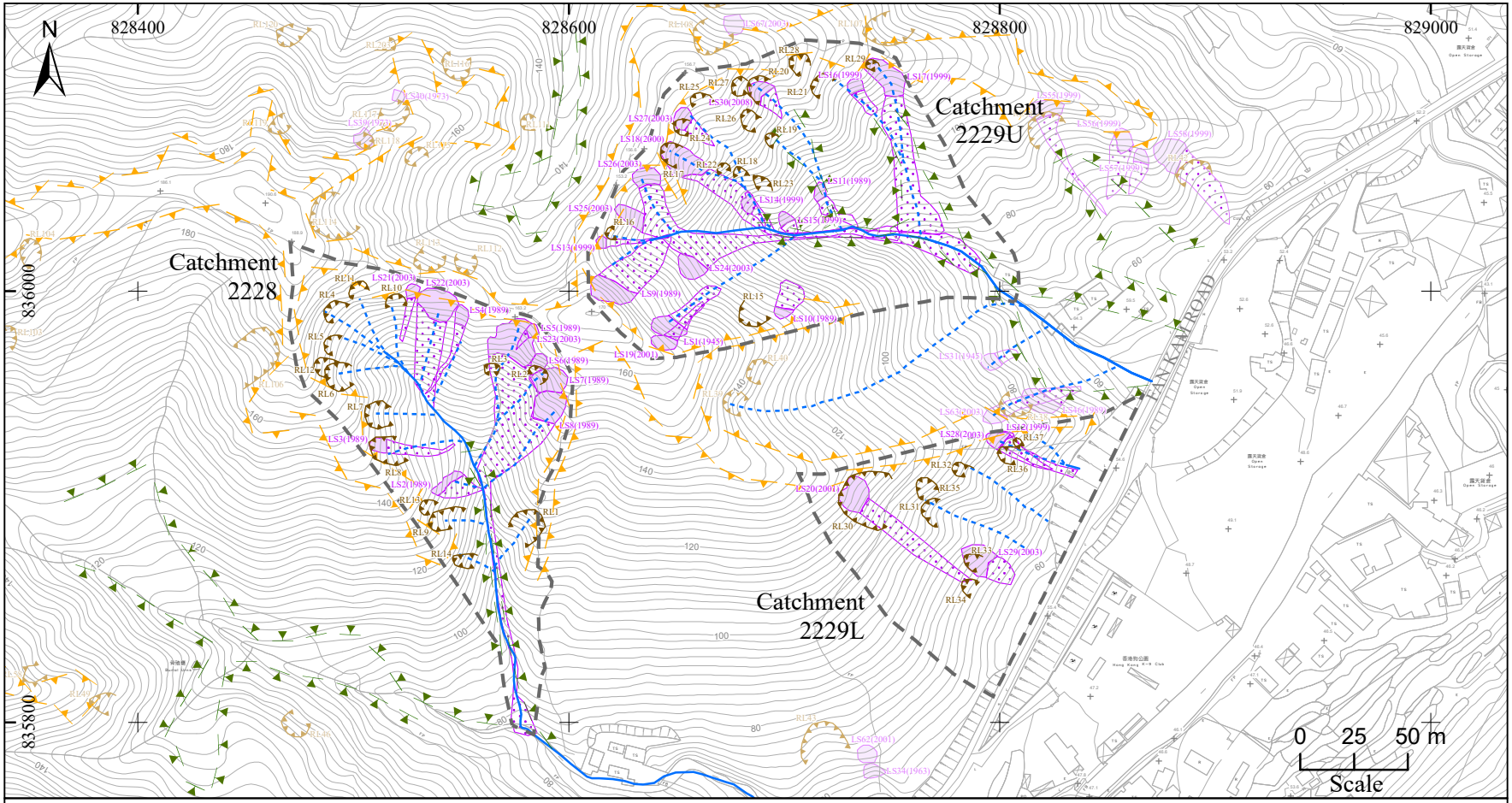

Figure A2 Past Instabilities and Geomorhpology

Appendix B

Landslide Mapping Plans

Contents

List of Figures

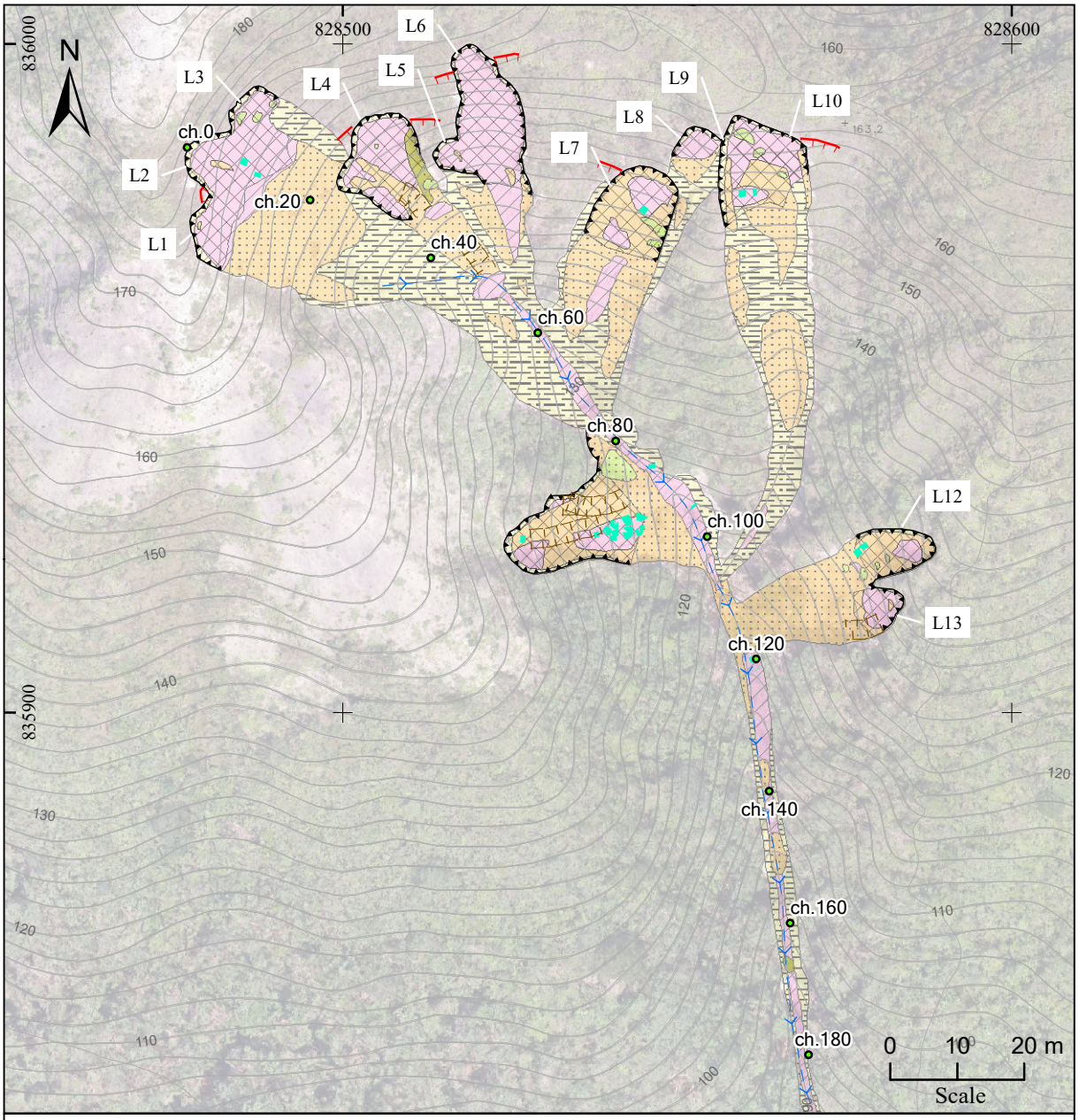

Legend:

- Crown of 2018 Landslide
- Central Main Drainage Line
- Gully
- Quartz Vein
- Tension Crack

Material Type

- MT1 Top Soil/ Colluvium
- MT2 Tuff
- MT3 Remoulded Debris
- MT4 Intact Debris Raft
- MT5 Clast Debris

Processes

- Source
- Transportation
- Entrainment
- Deposition

Note: Base plan is extracted from 1:1000 survey sheet Nos. 2SE-24D, 2SE-25C, 6NE-4B and 6NE-5A dated August 2014.

Figure B1 Plan of Sources and Upper Trail of Landslide Cluster 2228

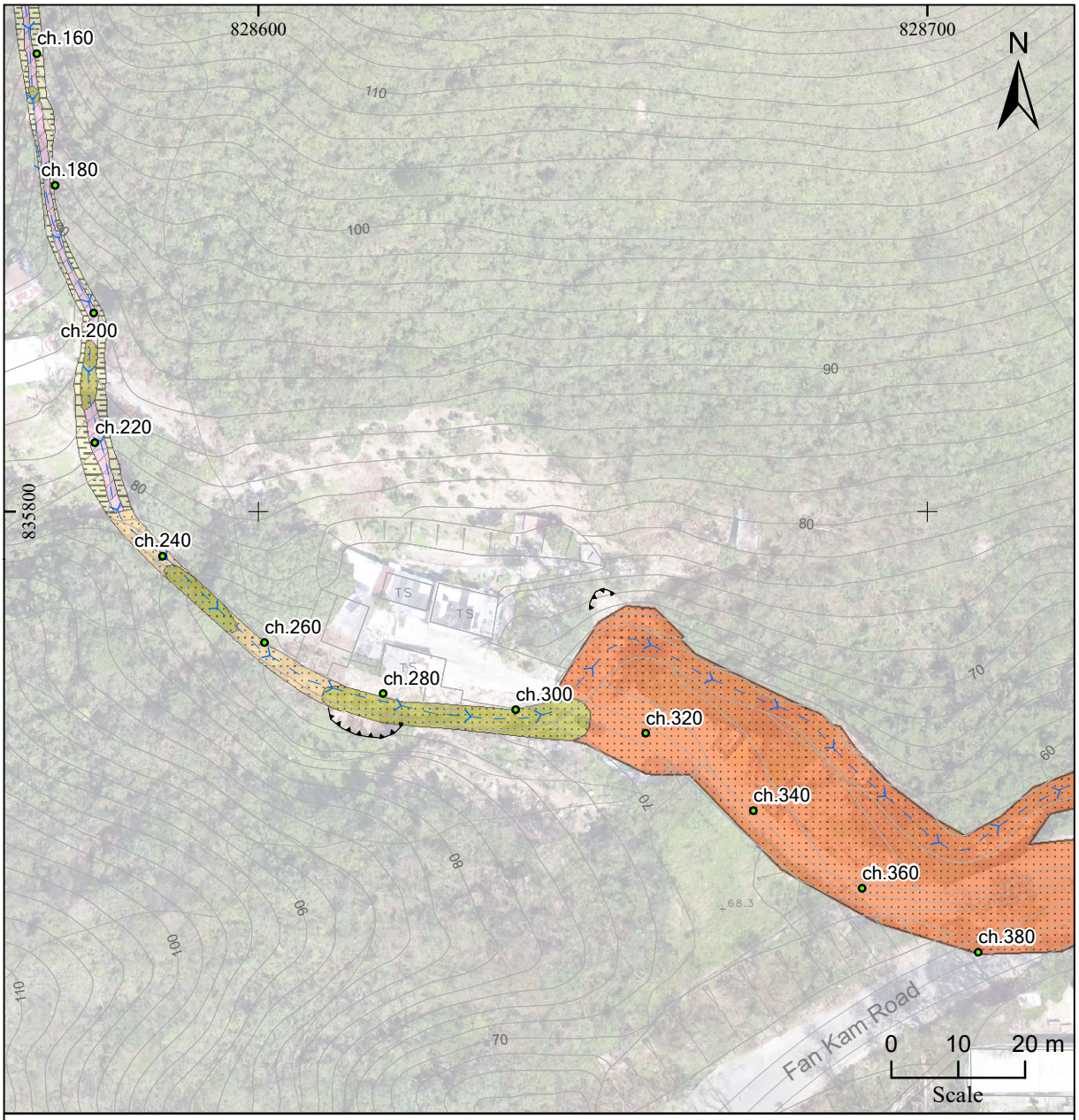

Legend:

Crown of 2018 Landslide

Central Main Drainage Line

Material Type

MT1 Top Soil/ Colluvium

MT2 Tuff

MT3 Remoulded Debris

MT5 Clast Debris

MT7 Outwash Debris

Processes

Transportation

Entrainment

Deposition

Note: Base plan is extracted from 1:1000 survey sheet Nos. 2SE-24D, 2SE-25C, 6NE-4B and 6NE-5A dated August 2014.

Figure B2 Plan of Lower Trail of Landslide Cluster 2228

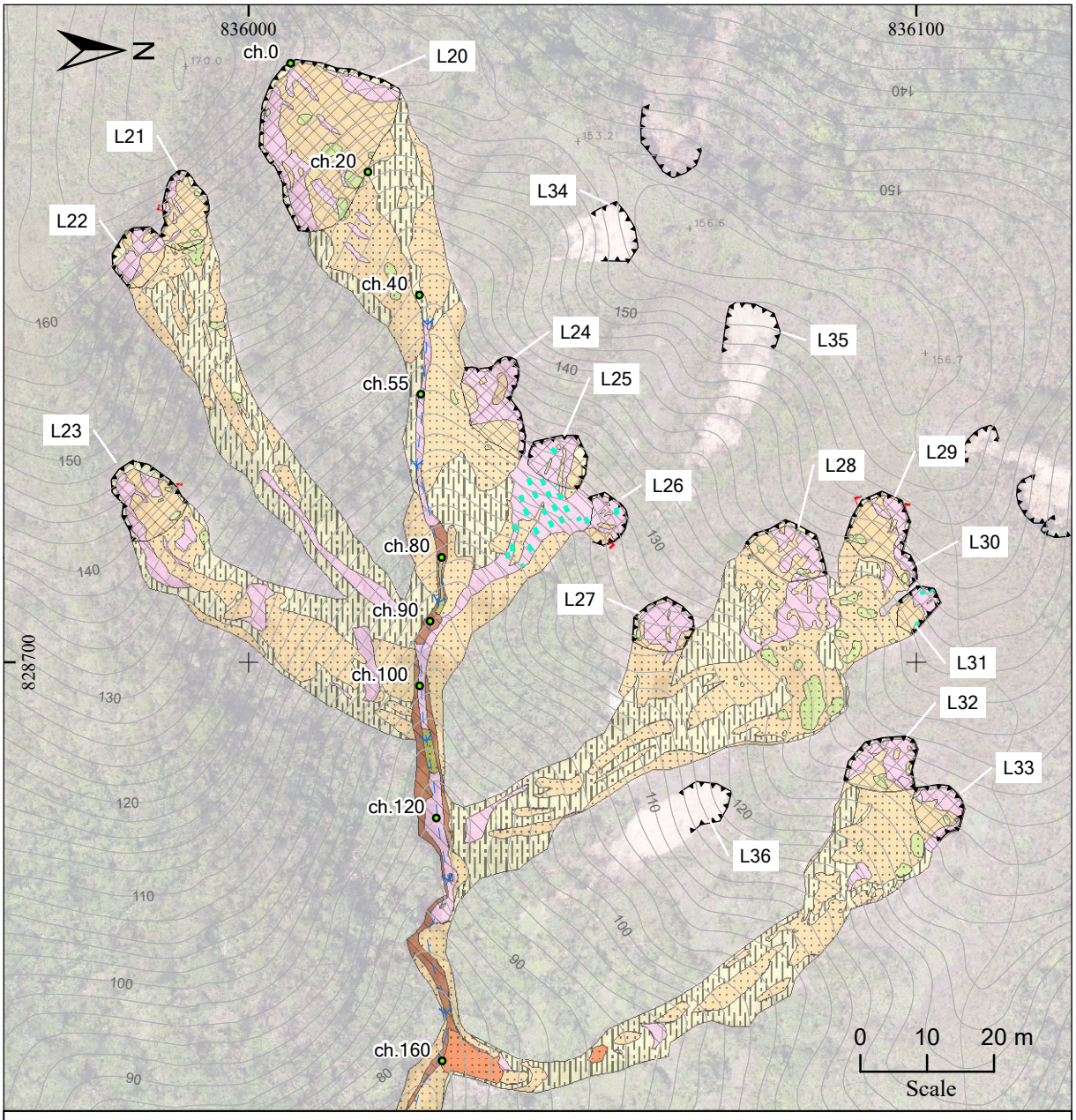

Legend:

- Crown of 2018 Landslide
- Central Main Drainage Line
- Tension Crack
- Quartz Vein

Material Type

- MT1 Top Soil/Colluvium
- MT2 Tuff
- MT3 Remoulded Debris
- MT4 Intact Raft Debris
- MT5 Clast Debris
- MT6 Valley Colluvium
- MT7 Outwash Debris

Processes

- Source
- Transportation
- Entrainment
- Deposition

Note: Base plan is extracted from 1:1000 survey sheet Nos. 2SE-25C and 6NE-5A dated August 2014.

Figure B3 Plan of Sources and Upper Trail of Landslide Cluster 2229U

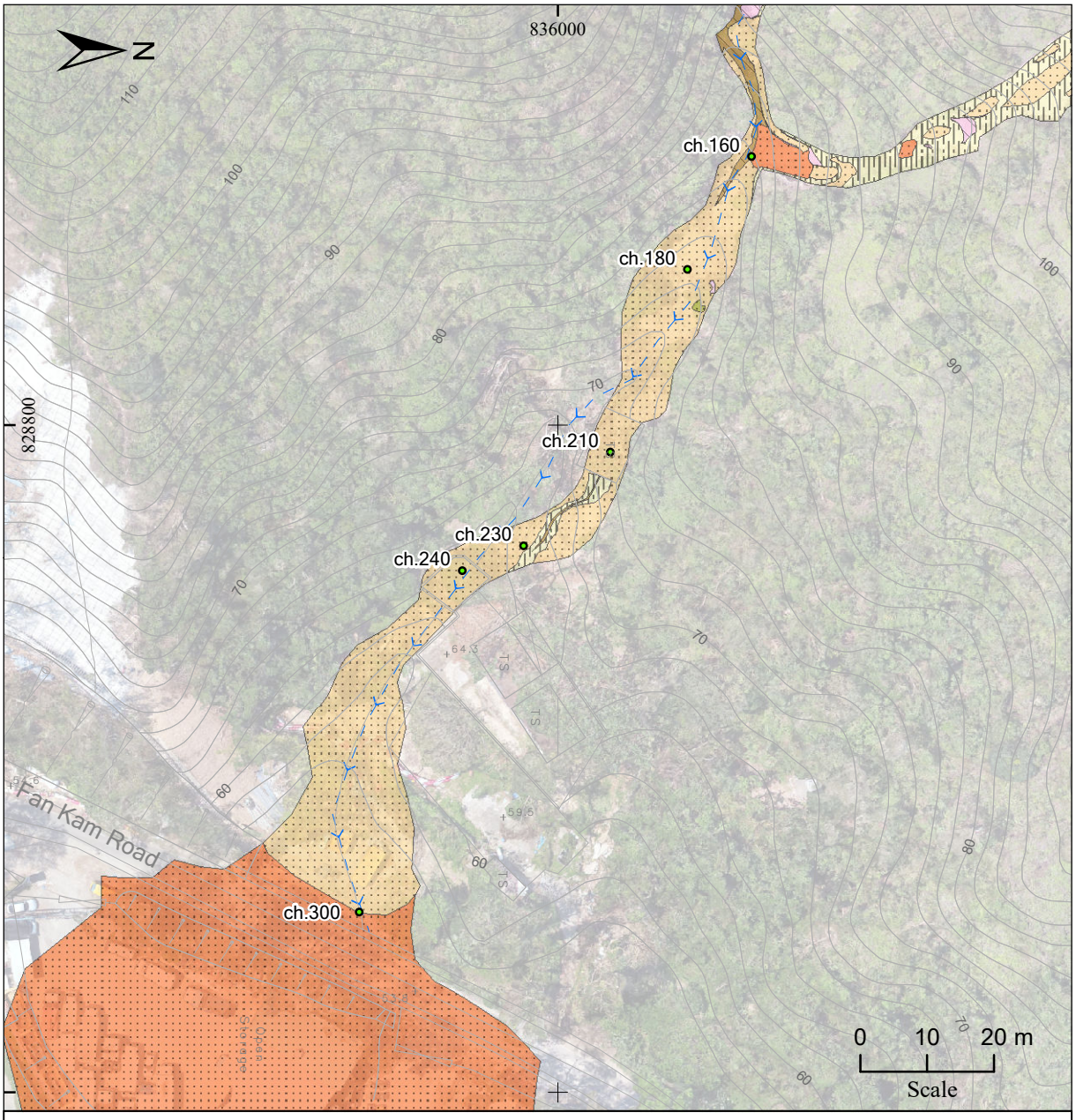

Legend:

Central Main Drainage Line

Material Type

- MT1 Top Soil/Colluvium
- MT2 In-situ Material
- MT3 Remoulded Debris
- MT5 Clast Debris
- MT6 Valley Colluvium
- MT7 Outwash Debris

Processes

- Transportation
- Entrainment
- Deposition

Note: Base plan is extracted from 1:1000 survey sheet Nos. 2SE-25C and 6NE-5A dated August 2014.

Figure B4 Plan of Lower Trail of Landslide Cluster 2229U

Appendix C

Diagnosis of the Probable Causes of Landslide Clustering

Contents

List of Table

List of Figure

C.1 General

Under an intense rainstorm, numerous landslides may occur on a hillside particularly in the susceptible areas. These landslides may develop into landslide clusters if the susceptible areas are closely spaced or connected. Notably, many 2018 landslides on the hillside above Fan Kam Road occurred in close proximity or with the scars/trails merged in some cases forming three distinct landslide clusters. A site-specific assessment has been conducted with a view to identifying the factors concerning landslide susceptibility of the subject hillside that could have caused landslide clustering (referred to as 'clustering factors' hereafter). Details of the assessment are presented in this Appendix.

C.2 Methodology of the Assessment

As revealed by Section 10.1 of the report, the continuous steep terrain evolved from the on-going geomorphological process, most areas also coupled with a high density of heads of drainage lines and past landslides, could have been a prominent predisposing factor to the 2018 landslides and hence the landslide clustering. Apart from the unique morphological characteristics, the adverse geological settings, viz. the presence of regolith susceptible to landslide initiation and possible adverse geological implication associated with regional fault activity, might similarly pose certain effect contributory to the landslide clustering. In order to provide insights on the certainty of this hypothesis on the clustering factors, testing has been carried out by comparing the characteristics and landslide responses of the landslide cluster areas with those of the other parts of the hillside. It is noted that anthropogenic activities might have played a part in only a small fraction of the landslides and their effect on landslide clustering is considered not particularly significant. Hillfire has also been assessed to have minimal effect on the landslides. As such, these two factors are not considered further in the testing.

Based on field mapping, API, review of UAV images and GIS analysis, two levels of testing have been conducted with a view to ascertaining the aforesaid hypothesis on the clustering factors:

(a) Level 1 Testing: Identifying landslide cluster areas over the hillside, reviewing the relevant characteristics and generalising the potential clustering factors.

(b) Level 2 Testing: Identifying areas over the hillside showing no evidence of landslide clustering yet with morphological characteristics similar to those at the landslide cluster areas, reviewing the relevant characteristics and exploring the degree of influence of the potential clustering factors identified from the Level 1 testing.

For the context of the assessment, the hillside area up to the summit of Kai Kung Leng has been studied. The boundary of this hillside area together with the Level 1 and Level 2 test areas are presented in Figure C1. With a view to better reflecting the landslide susceptibility, the consideration of landslide clustering has taken into account both the recent

landslides recorded in the Enhanced Natural Terrain Landslide Inventory (ENTLI) and the 2018 landslides (for simplicity referred to as 'past recent landslides' hereafter). For the purpose of the testing, a landslide cluster area is defined as where three or more past recent landslides occurred within a buffer of 30 m radius and its adjoining areas with reference to the methodology outlined in Lo & Ko (2017).

C.3 Testing Details and Salient Observations

Under the Level 1 testing, a total of seven landslide cluster areas on the hillside have been identified. These comprise the three distinct landslide cluster areas 2228, 2229U and 2229L plus another four areas (namely TA1-1 to 4) with landslide clustering of smaller scale (up to seven past recent landslides in each area). The seven areas are generally located around prominent convex break-in-slopes close to the ridgelines and at the lower part of the hillside close to Fan Kam Road where the regional Tai Lam Fault is aligned. Table C1 presents the characteristics and landslide responses of these landslide cluster areas. These areas typically involve steep terrain with gradient between 30° and 40° and presence of multiple heads of drainage lines in close proximity (viz. on average spaced within 30 m). Notably, a high portion of the past recent landslides within these areas came close to each other and located close to the heads of drainage lines. In respect of the geological settings, all seven areas are overlain by colluvium (while two areas are also overlain by some saprolite) within which the past recent landslides predominantly involved. The possible adverse geological implication associated with regional fault activity as inferred from the intensity of quartz is judged to be high to moderate in most cases.

The Level 1 testing establishes that the clustering factors hypothesised in Section C2 above (viz. steep terrain, high density of heads of drainage lines, presence of regolith susceptible to landslide initiation and possible adverse geological implication associated with regional fault activity) could be statistically correlated with the landslide clustering. With a view to exploring the degree of influence of the clustering factors identified, the Level 2 testing has been undertaken.

Under the Level 2 testing, eight areas on the hillside (namely TA2-1 to 8) showing no evidence of landslide clustering yet with morphological characteristics similar to those at the landslide cluster areas (viz. areas of gradient steeper than 30° with a high density of heads of drainage lines typically spaced within 30 m) have been identified for testing. Incidentally, these eight areas also broadly conform to the zone of prominent convex break-in-slopes close to the ridgelines but are located at higher elevation and farther away from Fan Kam Road as compared with the seven landslide cluster areas.

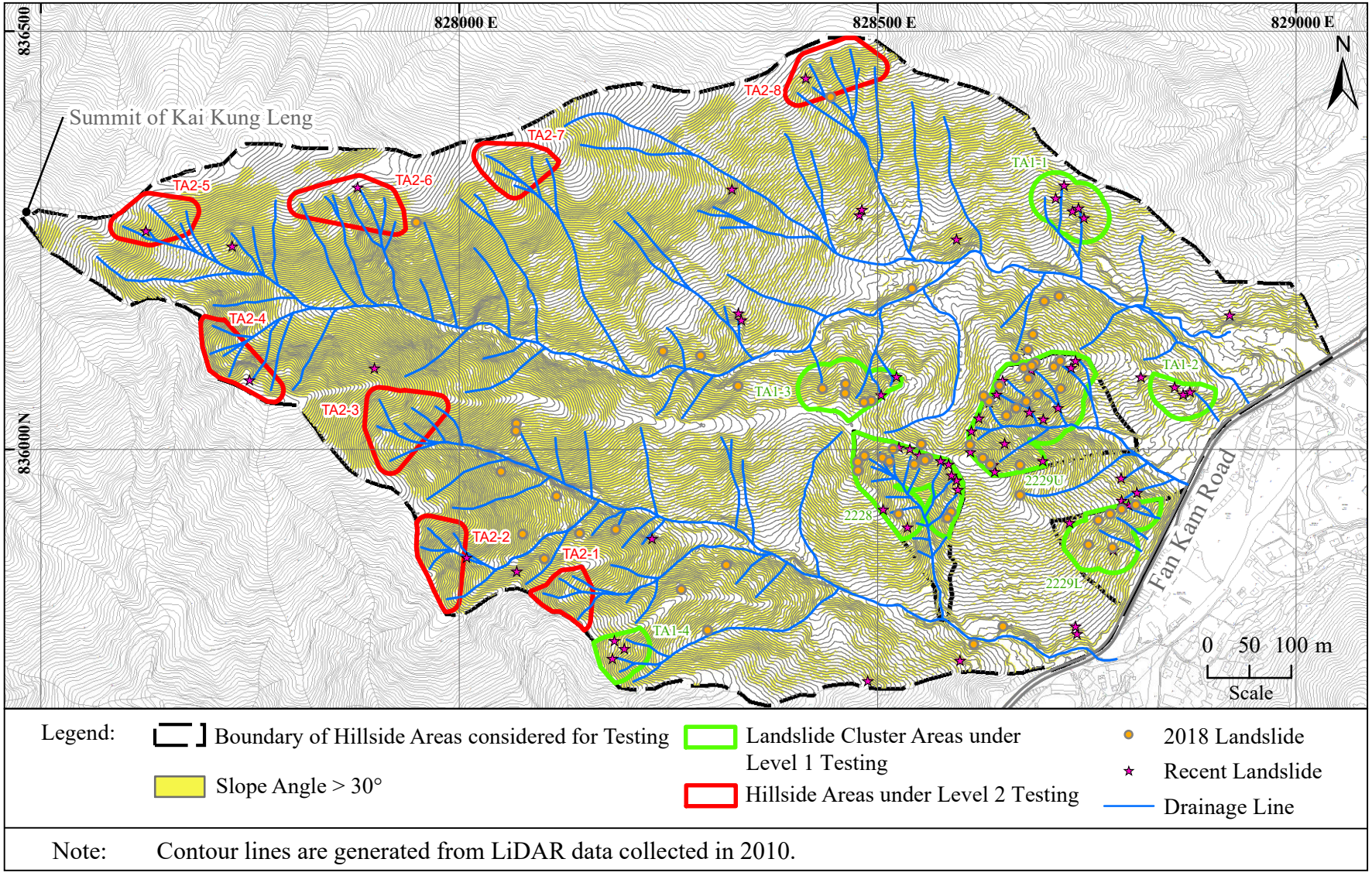

Figure C1 Locations of Level 1 and Level 2 Test Areas

Table C1 Characteristics and Landslide Responses of Landslide Cluster Areas under the Level 1 Testing and Hillside Areas under the Level 2 Testing

Area No.	Number of Past Recent Landslides	Average Slope Gradient Across the Areas (Degrees)	Number of Head of Drainage Line	Average Spacing of Head of Drainage Line (m)	Dominant Regolith Type	Intensity of Quartz (High / Moderate / Low)
Landslide Cluster Areas under the Level 1 Testing						
2228	23	35	13	18	Colluvium	H
2229U	31	36	10	21		H
2228L	9	34	4	17		M
TA1-1	5	32	3	27	Colluvium / saprolite	M
TA1-2	3	30	1	-	Colluvium	M
TA1-3	7	33	4	26		H
TA1-4	3	35	3	19	Colluvium / saprolite	M
Hillside Areas under the Level 2 Testing						
TA2-1	0	35	5	22	Saprolite	M
TA2-2	0	38	5	29		L
TA2-3	0	37	6	29	Saprolite / rock outcrop	L
TA2-4	1	37	6	22		L
TA2-5	1	32	5	26		L
TA2-6	1	34	7	21		L
TA2-7	0	32	5	22		L
TA2-8	1	31	7	22		L

The geological influence within the eight Level 2 test areas has been assessed (see Table C1). The regolith within these areas primarily comprised saprolite and rock outcrop with colluvium of limited extent. The more resistant and less permeable materials in these areas as compared with those overlying the landslide cluster areas would tend to inhibit the initiation of landslides. In terms of the solid geology as revealed by the published geological map, the eight Level 2 test areas are mostly within the metamorphic band (except TA2-2 and 3) similar to that of the landslide cluster areas. Yet, there appears to be a comparably lower intensity of quartz in the eight areas as noted from field observations. With the reduced influence of quartz, any impact on the groundwater regime would be less. The lower degree of mineral concentration may also suggest the possible adverse geological implication associated with regional fault activity to a relatively lesser extent as compared with the landslide cluster areas.

In a broad sense, the aforesaid geological influence may be attributed to the fact that the landslide cluster areas are located much closer to Fan Kam Road where the regional Tai Lam Fault is aligned (Figure 2.2). Associated with the regional fault, there could be a higher degree of hydrothermal and metamorphic activities. With the fractured nature of the fault and influence of the activities associated with faulting, materials lying within the fault zones and their close proximity are typically relatively weaker. In addition, as revealed by field observations, the intensity of quartz, which could have an adverse effect on the groundwater regime of the hillside, is generally higher at the areas adjacent to Fan Kam Road. Such influence appears to have been manifested by the observed trend of having a significantly higher density of past recent landslides closer to Fan Kam Road which also sheds some light on the prominence of these factors being considered on landslide susceptibility. Findings from the Level 2 testing affirm that the presence of regolith susceptible to landslide initiation and possible adverse geological implication associated with regional fault activity are the other contributing clustering factors in addition to those related to morphology. This provides further insights on the certainty of the clustering factors hypothesised.

C.4 Summary

The findings of the assessment suggest that the development of landslide clustering over the hillside above Fan Kam Road is the result of a complex combination of interconnected factors controlling landslide susceptibility. The continuous steep terrain has evolved from an active geomorphological process, particularly for those areas over-steepened by the development of heads of drainage lines and past landslides. There also appears to be a tendency of landslide cluster to develop around the heads of drainage lines. The steep gradient coupling with the high density of heads of drainage lines promoted erosion and further instability and could have been a prominent predisposing factor to landslide clustering.

In addition, the adverse geological settings are considered to be the other factors contributing to the landslide clustering. This involves the presence of regolith susceptible to landslide initiation, viz. colluvium being weaker and more vulnerable to infiltration as compared with in-situ weathered materials. Besides, areas in close proximity to the regional Tai Lam Fault along Fan Kam Road may have a higher susceptibility to landslide clustering. Associated with the regional fault, there could be a higher degree of hydrothermal and metamorphic activities. With the fracture nature of the fault and influence of the activities associated with faulting, materials lying within the fault zones and their close proximity are typically relatively weaker. The relatively weaker materials together with the potential adverse effect on the groundwater regime associated with the notable intensity of persistent quartz veins in the insitu weathered materials adjacent to the fault could have contributed to the landslide clustering. Such influence appears to have been manifested by the observed trend of having a significantly higher density of past recent landslides closer to Fan Kam Road.

C.5 Reference

Lo, F.L.C. & Ko, F.W.Y. (2017). *Rainfall-based Correlation of Recent Landslides with Clusters of Relict Landslides (Discussion Note No. DN 2/2017).* Geotechnical Engineering Office, Hong Kong, 9 p.

GEO PUBLICATIONS AND ORDERING INFORMATION
土力工程處刊物及訂購資料

An up-to-date full list of GEO publications can be found at the CEDD Website http://www.cedd.gov.hk on the Internet under "Publications". The following GEO publications can also be downloaded from the CEDD Website:

i. Manuals, Guides and Specifications
ii. GEO technical guidance notes
iii. GEO reports
iv. Geotechnical area studies programme
v. Geological survey memoirs
vi. Geological survey sheet reports

詳盡及最新的土力工程處刊物目錄，已登載於土木工程拓展署的互聯網網頁http://www.cedd.gov.hk 的"刊物"版面之內。以下的土力工程處刊物亦可於該網頁下載：

i. 指南、指引及規格
ii. 土力工程處技術指引
iii. 土力工程處報告
iv. 岩土工程地區研究計劃
v. 地質研究報告
vi. 地質調查圖表報告

Copies of some GEO publications (except geological maps and other publications which are free of charge) can be purchased either by:

Writing to
Publications Sales Unit,
Information Services Department,
Room 626, 6th Floor,
North Point Government Offices,
333 Java Road, North Point, Hong Kong.

or

- Calling the Publications Sales Section of Information Services Department (ISD) at (852) 2537 1910
- Visiting the online Government Bookstore at http:// www.bookstore.gov.hk
- Downloading the order form from the ISD website at http://www.isd.gov.hk and submitting the order online or by fax to (852) 2523 7195
- Placing order with ISD by e-mail at puborder@isd.gov.hk

讀者可採用以下方法購買部分土力工程處刊物(地質圖及免費刊物除外):

書面訂購
香港北角渣華道333號
北角政府合署6樓626室
政府新聞處
刊物銷售組

或

- 致電政府新聞處刊物銷售小組訂購 (電話：(852) 2537 1910)
- 進入網上「政府書店」選購，網址為 http://www.bookstore.gov.hk
- 透過政府新聞處的網站 (http://www.isd.gov.hk) 於網上遞交訂購表格，或將表格傳真至刊物銷售小組 (傳真：(852) 2523 7195)
- 以電郵方式訂購 (電郵地址：puborder@isd.gov.hk)

1:100 000, 1:20 000 and 1:5 000 geological maps can be purchased from:

Map Publications Centre/HK,
Survey & Mapping Office, Lands Department,
23th Floor, North Point Government Offices,
333 Java Road, North Point, Hong Kong.
Tel: (852) 2231 3187
Fax: (852) 2116 0774

讀者可於下列地點購買1:100 000、1:20 000及1:5 000地質圖：

香港北角渣華道333號
北角政府合署23樓
地政總署測繪處
電話: (852) 2231 3187
傳真: (852) 2116 0774

Any enquires on GEO publications should be directed to:

Chief Geotechnical Engineer/Standards and Testing,
Geotechnical Engineering Office,
Civil Engineering and Development Department,
Civil Engineering and Development Building,
101 Princess Margaret Road,
Homantin, Kowloon, Hong Kong.
Tel: (852) 2762 5351
Fax: (852) 2714 0275
E-mail: ivanli@cedd.gov.hk

如對本處刊物有任何查詢，請致函：

香港九龍何文田公主道101號
土木工程拓展署大樓
土木工程拓展署
土力工程處
標準及測試部總土力工程師
電話: (852) 2762 5351
傳真: (852) 2714 0275
電子郵件: ivanli@cedd.gov.hk